Study of Sn-Zn Solder Alloy as A Conventional Sn-Pb Solder Replacement

by

Sazol Kumar Das

Submitted to

Department of Materials and Metallurgical Engineering in Partial Fulfillment of the Requirements for the Degree

of

MASTER OF SCIENCE IN MATERIALS AND METALLURGICAL ENGINEERING

Department of Materials and Metallurgical Engineering

BANGLADESH UNIVERSITY OF ENGINEERING AND TECHNOLOGY

OCTOBER 2008

The thesis entitled, "**Study of Sn-Zn Solder Alloy as A Conventional Sn-Pb Solder Replacement**" Submitted by Sazol Kumar Das, Roll No. 100611004F, Session: October, 2006 has been accepted as satisfactory in partial fulfillment of the requirement for the degree of Master of Science in Materials and Metallurgical Engineering on October, 2008.

BOARD OF EXAMINERS

(Ahmed Sharif)

Chairman

Dr. Ahmed Sharif
Assistant Professor
Department of Materials and Metallurgical Engineering
BUET, Dhaka-1000

( )

Member (Ex-officio)

Dr. Md. Fakhrul Islam
Professor and Head
Department of Materials and Metallurgical Engineering
BUET, Dhaka-1000

( )

Member

Dr. Md. Moniruzzaman
Associate Professor
Department of Materials and Metallurgical Engineering
BUET, Dhaka-1000

( )

Member (External)

Prof. Dr. M. Rezwan Khan
Vice-Chancellor
United International University
Road No. 8A, Dhanmondi, Dhaka

CANDIDATE'S DECLARATION

It is hereby declared that this thesis or any part of it has not been submitted elsewhere for the award of any degree or diploma

Signature of the Candidate

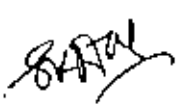

Sazol Kumar Das

DEDICATION

To my Father, Anil Chandra Das, who have been sources of strength, encouragement and inspiration throughout my life

and

To my Mother, Kallani Rani Das, without whose support, incentive and love, my education, my career and my personal life would have been much less.

TABLE OF CONTENT

List of Tables

List of Figures

List of Abbreviations

ACF	Anisotropic Conductive Film
BGA	Ball Grid Array
BOD	Biological Oxygen demand
BSE	Back Scattered Electron
CBGA	Ceramic Ball Grid Array
CCD	Charge Coupled Device
CFC	Chlorofluorocarbon
COD	Chemical Oxygen Demand
CTE	Coefficient of Thermal Expansion
DRAM	Dynamic Random Access Memory
DSC	Differential Scanning Calorimetry
EDX	Energy Dispersive X-ray
EPA	Environmental Protection Agency
EU	European Union
FC	Flip Chip
IC	Integrated Circuit
ICA	Isotropic Conductive Adhesive
ILB	Inner Lead Bonding
IMC	Intermetallic Compound
IML	Intermetallic Layer
I/O	Input output
IR	Infrared
JEITA	Japan Electronics and Information Technology Industries Association
NEMI	National Electronics Manufacturing Initiative
OM	Optical Microscope
OLB	Outer Lead Bonding
PBGA	Plastic Ball Grid Array
PCB	Printed Circuit Board

PTH	Pin Through Hole
PWB	Printed Wiring Board
QFP	Quad Flat Pack
R	Rosin
RA	Rosin Activated
RMA	Rosin Mildly Activated
RoHS	Restriction of Certain Hazardous Substances
SEM	Scanning Electron Microscope
SE	Secondary Electron
SMT	Surface Mount Technology
TAB	Tape Automated Bonding
TBGA	Tape Ball Grid Array
Tm	Melting Temperature
Top	Operating Temperature
UBM	Under Bump Metallization
UTS	Ultimate Tensile Strength
WEEE	Waste Electrical and Electronic Equipment

List of Notations

η	Homologous temperatures
τ	Stress at the particle surface
n	Piled-up dislocation number
τ_0	Yield stress of the alloy
L	Average distance between the second phase particles
b	Burgers Vector
ν	Poisson's ratio
G	Shear elastic modulus of the substrate

Abstract

Due to the inherent toxicity of lead (Pb), environmental regulations around the world have been targeted to eliminate the usage of Pb-bearing solders in electronic assemblies. This has triggered the development of "Pb-free" solders for the electronic industries. In order to become a successful solder material, Pb-free solder alloys need to be reliable over a long term. Even though many Pb-free solder alloys possess higher strength than the traditional Sn-Pb ones, there still exist some reliability problems such as low solderability and high interfacial reaction on metallization pad of packaging substrate. It is the aim of this study to develop new Pb-free solders and to characterize some of their thermal and mechanical properties.

In this study, the new Pb-free solders were developed by doping trace amounts of Al and Cu into Sn-9Zn eutectic solder. These solder alloys were Sn-9Zn-0.5Al and Sn-9Zn-0.7Cu. In general, the resulting Al-doped Pb-free solder was found to have better properties than the original Sn-9Zn eutectic solder.

The microstructures of all the Pb-free solders were refined and become more uniform with the addition of both Al and Cu. For instance, with the addition of 0.5wt% Al in Sn-9Zn, the coarse β-Sn grain size was reduced and the intermetallic compound (IMC) particles became finer in eutectic colonies. Since only trace amount Al was added into the eutectic Sn-9Zn solder, the melting temperatures were only slightly changed comparing with the eutectic melting temperature. It was also found that with slower cooling rate the microstructure of the Sn-9Zn solder contained thick eutectic lamella, i.e. rod-like α-Zn phase in the β-Sn matrix, while fast cooling resulted in a fine needle like α-Zn phase dispersed in β-Sn matrix more uniformly.

A change of microstructure in turn affected the mechanical properties of the solders. Thus when Sn-9Zn solder is doped with Al and Cu, for both cases the microhardness was improved due to formation of intermetallic compound. When Sn-9Zn solder was doped with a small percentage of Al, the tensile properties was also improved. The improvement in tensile strength was found to be traded off with the decrease in elongation.

Composite approach is a very new technique to improve the properties of Pb-free solder. Ag micro-particles content in the range between 0 - 4.0 wt.% with Sn-9Zn eutectic system, were examined in order to understand the effect of Ag addition on the microstructural and mechanical properties as well as the thermal behavior of the composite solders. The shear strengths and the interfacial reactions of Sn-Zn micro-composite eutectic solders with Au/Ni/Cu ball grid array (BGA) pad metallization were systematically investigated. The three distinct intermetallic compound (IMC) layers were formed at the solder interface of the Au/electrolytic Ni/Cu bond pad with Sn-Zn composite alloys. The more Ag particles added to the Sn-Zn solder, the more Ag-Zn compound formed to thicken the uppermost IMC layer. The dissolved Ag-Zn IMCs formed in the bulk solder redeposited over the initially formed interfacial Au-Zn IMC layer, prevented the whole IMC layer lift-off from the pad surface. Cross-sectional studies of the interfaces were also conducted to correlate with the fracture surfaces.

Acknowledgement

First and foremost, I would like to express my special gratitude to my supervisor Dr. Ahmed Sharif, who has provided me with invaluable guidance and support throughout this work. Dr. Sharif has given me continuous help, encouragement and opportunity, without which I could not have completed this thesis.

Heartfelt thanks are extended to Professor Y. C Chan City University of Hong Kong for his great input and support during my stay at City University of Hong Kong.

I am grateful to all the teachers and staffs in the MME Department, Bangladesh University of Engineering and Technology for their help and assistance.

Special thanks to the colleagues in the EPA centre, City University of Hong Kong for their help and assistance during my stay there.

I wish to dedicate this dissertation to my family for their wholehearted backing and understanding.

I would like to acknowledge the financial support provided by the CASR of Bangladesh University of Engineering and Technology and Research Grant Council of Hong Kong for the CERG project no. CityU 111307 (CityU ref. 9041222)

CHAPTER 1

INTRODUCTION

1.1 INTRODUCTION TO ELECTRONIC PACKAGING

1.1.1 Trend of Electronic Industry

The invention of the transistor in 1947 revolutionized the semiconductor industry as it enabled the size of electronic products to decrease considerably. In order to achieve high functionality and high performance in products, the integrated circuit (IC) technology was developed in the early 1960's to integrate several transistors on a single semiconductor chip [1]. The continuous advances in decreasing the size of the transistors have provided the progressive integration of hundreds, then thousands of transistors on a single IC chip. Since then, electronic products have become smaller and smaller, and progressively more functional. This helped to bring the electronics market to become one of the largest industries in the world, surpassing the worldwide steel and automotive industries, as shown in Figure 1.1 [2]. It is envisaged that with the present growth in portable consumer electronic products, the electronics market will continue to grow.

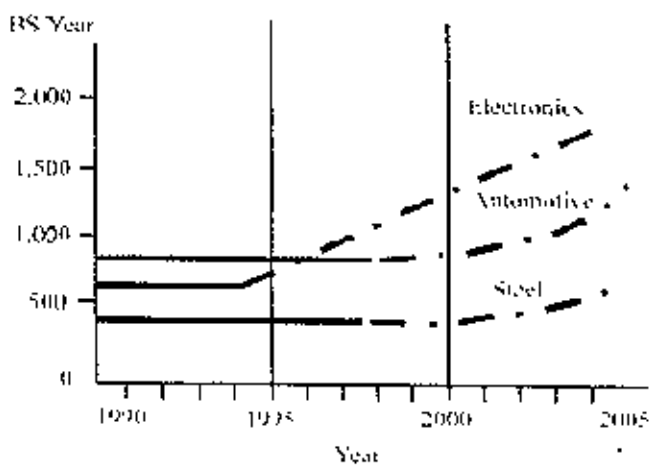

Figure 1.1 Trend of electronic industry, automotive & steel [2].

1.1.2 What are Electronic Packaging and Assembly?

After the IC fabrication process is finished on the wafer, the wafer is cut into individual ICs or chips by using a diamond blade. To be able to use these ICs, they have to be packaged and tested to guarantee the functions and quality of the ICs. The functions of an IC package are to protect and provide power to the ICs so that the ICs can be electrically connected and mechanically supported between the parts and the outside world. In other words, the input/output (I/O) connection pads on the IC are connected to the corresponding terminal pads on the package so that electronic signals pass in and out of the IC through the I/O connections. When the packaged ICs are interconnected to other electronic components, such as transistors and capacitors, on a system board, it is called the assembly process. This is always involved at the system level.

During the packaging and assembly processes, electronic solder is the prime material used for the interconnections between chip and package or between packaged IC and circuit board. The conventional solder is eutectic binary Sn-37Pb alloy, which has a single melting temperature of 183°C and possesses good mechanical properties as well as wettability. This material has been used in electronics production without too much major problem. However, the recent increase in the awareness of environmental and health concerns have caused the decision in many parts of the world to ban the use of Pb-bearing solders in electronics production. Hence, development of Pb-free solders is an urgent task.

1.2 PACKAGING HIERARCHY

Bonding the die or chip to a substrate with encapsulation is referred to as Level 1 packaging [3]. The usual method of electrical connection to the chip is through wire bonding or the use of solder bumps. A more modern approach is through the flip chip configuration as shown in Figure 1.2. The silicon die is turned "upside down" and mounted on the substrate.

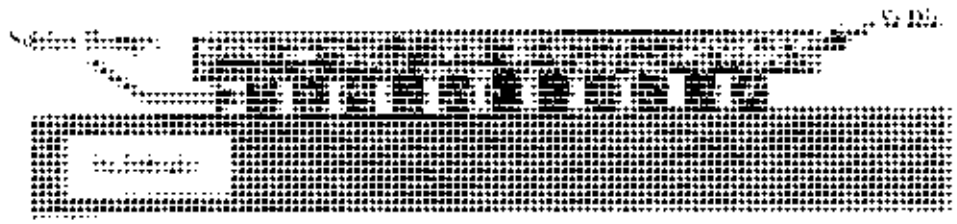

Figure 1.2 Cross-section of a flip chip connection.

Level 2 packaging is the interconnection of components, including the encapsulated silicon die, on a substrate carrier such as a printed wiring board (PWB). The eutectic Sn-37Pb solder has been the main material for interconnection at Level 2 packaging. The packaged product is commonly referred as "cards". There are two primary methods to attach electronic components to PWBs. They are pin-through-hole (PTH) and surface mount technology (SMT) as illustrated in Figures 1.3 and 1.4 respectively.

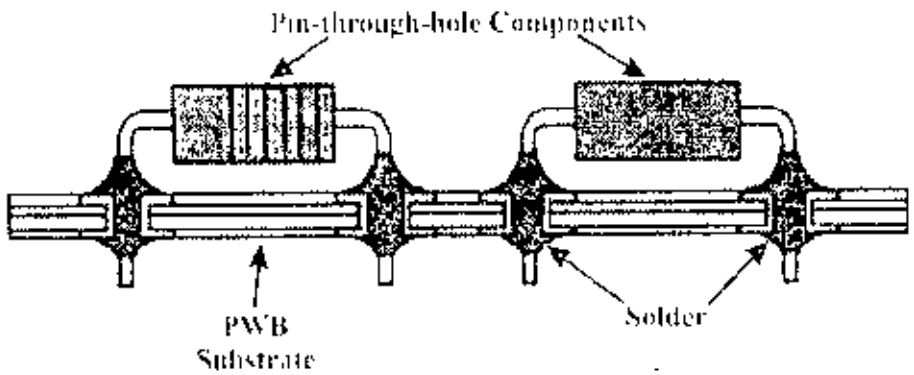

Figure 1.3 Cross-section of a pin-through-hole connection on a printed wiring board.

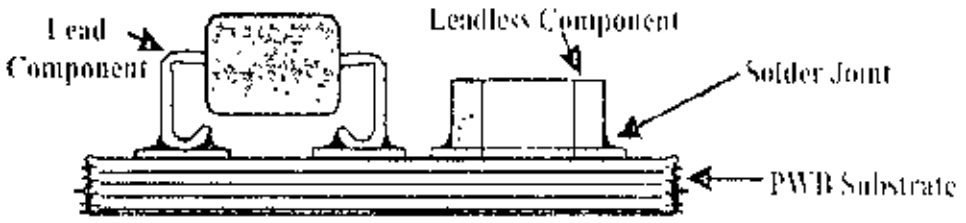

Figure 1.4 Cross-section of a surface mount connection on printed wiring board

The PTH assembly is done by inserting the component leads into plated holes in the PWB and soldering them. The soldering operation can be performed using either a wave soldering or a common solder iron. The components can be fixed by clinching the leads on the backside of the board before passing through the wave soldering machine. Component insertion can be done either manually or automatically. The PTH assembly demand has dropped significantly in the last decade due to the increase in production cost for drilling holes on PWB.

With SMT assembly the components, lead or leadless, are placed on a surface of PWD, rather than inserting them through the holes. To facilitate soldering, solder paste is first screen-printed on the pads of the board by stencil-printing. The components are then placed on the board, followed by heating the solder paste to form solder joints in the reflow oven. It is possible to glue the surface mount components to the board and solder them by wave soldering. However, this technique is commonly used when PTH and SMT components are involved on the board.

Level 3 packaging refers to the integration of many PWBs or cards to form a complete system. For example, a personal computer is composed of a mother board, a sound card and display card, etc

1.3 TYPES OF PACKAGING METHODS

1.3.1 Wirebonding

Wirebonding, a chip-to-package interconnection technique, is involved at Level 1 packaging. In this process, a chip is attached on the carrier. A fine metal wire, typically gold (Au) wire of 25 μm in diameter, is attached between each of the I/O pads on the chip and its associated package pin one by one at a time, as shown in Figure 1.5. The Au wire is ultrasonically bonded between the IC bond pad and the corresponding package or substrate bond pad. The package is encapsulated by epoxy to provide mechanical support and environment protection. Since wirebonding is a slow interconnection process and requires large pitch size, tape automated bonding (TAB) is developed to save time and production cost.

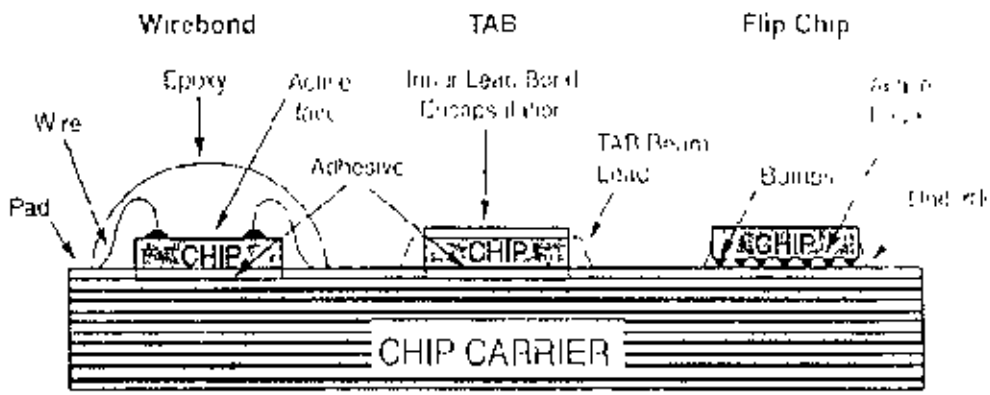

Figure 1.5 Chip to package or carrier interconnection techniques.

1.3.2 Tape Automated Bonding (TAB)

TAB is a Level 1 packaging process. Typically, a chip is joined to a patterned or metallized flexible polymer tape, such as copper on polyamide. In a TAB process, there are two types of bonding, i.e. Inner Lead Bonding (ILB) and Outer Lead

Bonding (OLB) With ILB, the chip and patterned copper leads are interconnected by thermo compression. This is followed by OLB, in which the other end of the patterned copper leads is interconnected to the PWB or substrate using Level 2 packaging techniques A common encapsulation process is also employed onto the chip as shown in Fig 1.5

Another feature of TAB is the bumping requirement for ILB. The interconnection between the chip and the inner leads are formed by the cushion effect of the bump. The bump provides both the necessary metallurgy for the ILB and a physical standoff to prevent lead-chip shorting. A bump material is usually pure Au or Sn-Pb solder applied by electro deposition Pure Au bumps are more popular than solder because the compliance of Au bumps is higher than that of solder [4]. It is a normal practice to build the Au bumps on under bump metallization (UBM) of the chip. This will be discussed in the following section.

1.3.3 Flip Chip (FC)

FC interconnection is the connection of an IC chip to a carrier or substrate with the active face of chip facing toward the substrate, as illustrated in Figure 1.5. The interconnection between the chip I/O and substrate is achieved by using a FC bump structure The functions of the FC bump are to provide the electrical and mechanical connections between the chip and the substrate. It also acts as a heat dissipation path from the chip.

The FC interconnection system can be subdivided into four functional areas: (1) under bump metallization (UBM), (2) chip bumps, bond materials between the bump and substrate metallization, (3) underfill encapsulant, and (4) substrate metallization. A schematic is shown in Figure 1.6.

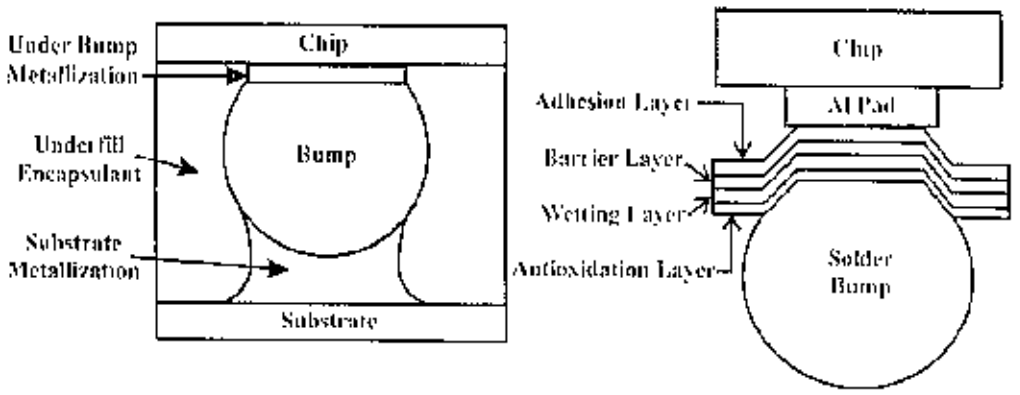

Figure 1.6 Schematic diagram of the flip chip interconnect system

The UBM serves as a compatible layer between the final chip metallization and the substrate metallization. The most common final chip metallization is aluminum (Al) or copper (Cu); while the substrate metallization is Au/Ni layer. The UBM also helps prevent the corrosion of the chip metallization due to diffusion of contaminant ionic from the under-fill encapsulant.

The structure of the UBM consists of four sputtered layers. The first layer is the adhesion layer, typically chromium (Cr), titanium-tungsten (TiW), etc. deposited directly on the final chip metallization. It provides good adhesion and acts as high strength and low contact resistance between the final chip metallization and the bump. The second layer is the barrier layer, which can be chromium-copper (Cr-Cu), nickel (Ni), etc. to be deposited over the adhesion layer. The barrier layer prevents diffusion of metal atoms to be deposited thereafter into the Al pad. After the barrier layer, there is a wetting layer. This is a consumable layer for the subsequent bump to provide wetting reaction to form intermetallic compounds. The typical wetting layer material is copper (Cu) or Ni. The final UBM layer is an antioxidation layer, which is optional, and is usually a very thin Au layer. The Au thickness needs to be small to avoid embrittlement of the UBM-bump interface.

The most common bump material is Sn-Pb solder, especially high melting temperature ones. High lead solder, e.g. 5wt%Sn-95wt%Pb, has melting point of ~300°C. Using the high temperature solder at Level 1 packaging prevents re-melting of the solder bumps when Level 2 packaging is carried out. The solder bumps are usually deposited by evaporation or electroplating onto the UBM structure.

1.3.4 Ball Grid Array (BGA)

The size and performance limitations of peripherally-leaded packages like the quad flat pack (QFP) are generally overcome by the BGA package. The BGA is an area array interconnection method, in which the I/O terminals are formed by an array of solder balls located well within the boundaries of the package, for bonding to the next level of package such as PWB. The difference between peripheral and area array is shown in Figure 1.7. The pitch means the center-to-center spacing between pads or rows of bumps solder balls

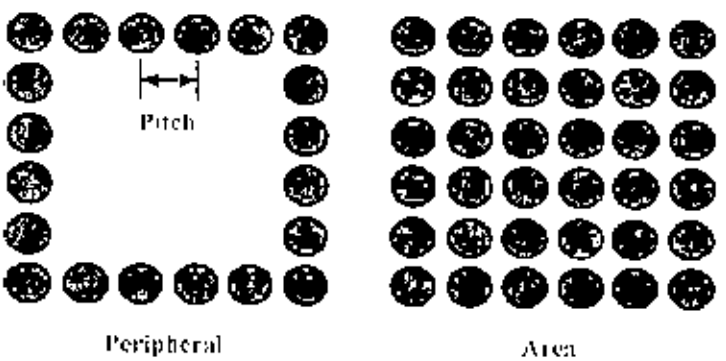

Figure 1.7 I/O difference between peripheral & area array.

In general, there are three broad groups of BGA's: plastic (PBGA), ceramic (CBGA), and tape (TBGA), based on the substrate materials used. The BGA is the most popular packaging method for advanced microelectronic applications. It is because an area array of solder balls allows for easy expansion of I/O terminals by increasing the I/O ball count while maintaining the I/O pitch. When the BGA concept is

applied on FC technology, very high I/O counts can be achieved for high performance electronic products.

1.4 INTERCONNECTION MATERIALS

The aim of soldering is to get an electrical, mechanical and thermal connection between the components and the PWB. The basic material required to create a good solder joint are solder and flux. At the interface of the solder joint, an intermetallic compound layer (IML) is formed between the pad and the solder. This section will discuss the roles of different interconnection materials.

1.4.1 Solder, Flux and Solder Paste

The conventional solder is the eutectic binary alloy of Sn and Pb (63wt%Sn-37wt%Pb), or a near eutectic composition, e.g. 60wt%Sn-40wt%Pb. They are popular to be used in PTH and SMT assemblies because of attributes of low cost, low melting temperature (183°C), and high reliability to join common assembly metals. Also, the surface mount components are self-aligned on the pads during soldering. Due to environment and health concerns, it is expected that Pb-bearing solders are eliminated or will be eliminated from electronic assemblies. So, commercially available Pb-free solders are obviously needed to achieve this.

The purpose of the flux is to reduce the surface oxides from both the molten solder and the substrate to be soldered [5]. Also, the flux will prevent the formation of fresh oxide on both solder and substrate during soldering so that formation of intermetallic compound between solder and substrate acts as chemical joint. When choosing the type of flux to be used, the melting temperature of the solder, the surface finishes on the component lead and on the solder pad, together with the activity of the flux should be considered. In general, fluxes are classified according to their activity level:

1.R (rosin), water-white rosin in organic solvents, without activators.

2.RMA (rosin mildly activated): similar to R, but mildly activated.

3.RA (rosin activated), similar to R, but the most active and corrosive.

After the soldering process, the residual flux on the surface of the assembly should be cleaned by water or organic solvent to avoid leakage currents, ionic migration between neighboring conductors (formation of dendrites), and corrosion. The more up-to-date soldering process employs "no-clean" flux to lessen the amount of environmentally unfriendly waste. Moreover, the production cost and processing time are also reduced.

Electronic solders usually come in the form of bars and pastes. Solder bars are solder alloy cast into a bar shape. They are normally used in wave soldering; while solder pastes are screen-printed or stencil-printed on the pads before reflow soldering. The solder paste consists of small solder spheres, flux and solvent. The solder spheres are usually eutectic Sn-Pb or Pb-free alloys, which is a homogeneous mixture in a flux medium. The solvent is an activator and a viscosity regulating agent. Therefore it is a thick gray paste with adequate viscosity to attach the components on the board during reflow process.

1.4.2 Inter metallic Compound Layer (IML)

The IML formation is inevitable at the interface between the pad and the solder during soldering. The formation of this layer is due to the wetting reaction between the solder and substrate above the melting point of solder for times of about 1 min [6]. After formation, the IML can grow either by a solid-state reaction below the melting temperature of solder, or by liquid-solid reaction above the melting temperature of solder. The IML growth depends on temperature and time. For most microelectronics applications, the solder is normally Sn-based. So when applied on Cu, the IML formed is normally Cu_6Sn_5. Excessive IML growth will deteriorate the joint strength due to its brittle characteristics. Hence, the interfacial interaction may affect the long-term reliability of solder joint.

1.4.3 Conductive Adhesive Materials

Conductive adhesive materials are usually used for bonding between the Au bump and substrate metallization during FC packaging. There are two major conductive adhesives (1) isotropic conductive adhesive (ICA) and (2) anisotropic conductive film (ACF) as shown in Figure 1.8a and b, respectively.

The ICA is typically thermosetting polymer filled with conductive particles. The most common material used is epoxy filled with silver flakes. It provides approximately equal electrical conductivity in all directions upon curing. The function of the polymer matrix is for the adhesion between the bump and the substrate metallization. Also, it prevents the corrosion of the conductive particles from the outside environment. To obtain isolation between adjacent pads, the ICA is screen or stencil printed only on the contact pads. Au bumping is most commonly used because it minimizes corrosion of the interconnection system. The underfill material can be applied to the interconnection system and simultaneously cured with the ICA. The ICA does not provide self-alignment during assembly like solders, leading to the requirement of high precision assembly tools.

The ACF has a similar function and structure to the ICA. It usually comes in either the paste-type or a film-type polymer filled with conductive particles. These conductive particles are metal-coated (Au or Ni/Au) polymer spheres with 3-5μm diameter, and then coated with a final insulating layer that protects them against shorting through contact with a neighboring particle. The ACF only conducts electric current when the conductive particles are compressed and captured between the bump on the IC and the substrate metallization, as shown in Figure 1.8b. During the assembly process, appropriate heat, pressure and holding time are applied to the ACF. Under these conditions, the epoxy is melted, while conductive particles are deformed and trapped between the Au bump and substrate metallization so that only z-direction electrical conductivity is possible. An uncompressed ACF serves as encapsulation behavior. Similar to ICA, ACF does not provide self-alignment like

solder. A high accuracy component placement is required during the assembly process

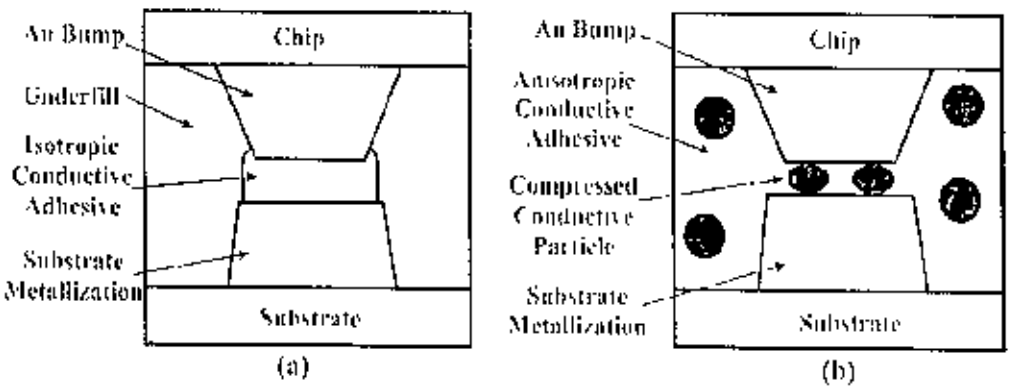

Figure 1 8 Schematic diagrams of (a) ICA and (b) ACF.

The advantages of using ICA and ACF are as follows

Firstly, die use of conductive adhesive eliminates the Pb usage in conventional solder and is therefore environmentally friendly. Secondly, it has a lower processing temperature than solder In general, the soldering temperature of Sn-Pb solder is about 235°C. However, die curing temperatures of the ICA and ACF are about 150°C and 180°C, respectively. As a result, energy is saved and production cost is reduced form the viewpoint of the electronic industry

However, joint resistance instability and adhesive strength variation are disadvantages of using ICA during under-curing state. It is because ICA pastes have low electrical conductivity before curing; while conductivity increases dramatically when the ICA is cured. Inadequately cured ICA can absorb a significant amount of moisture, causing oxidation on the adhered surface. Even though very stable adhesives have become available, the resistance of the joint increases after temperature and humidity aging. As a result, the resistance of the joint may become unstable. Apart from this, the ICA may be under-cured or over-cured. Since ICA usually has a thermosetting polymer matrix, polymer chains are grown and branched to form three-dimensional crosslink structure, allowing this polymer to be more rigid

with higher strength than a thermoplastic polymer. An under-cured ICA does not have sufficient cross-links inside the adhesive such that its cohesive strength may be weak. Also, it may absorb excessive moisture. Over-cured ICA may lead to too many cross-links generated inside the adhesive. Consequently, this adhesive becomes brittle and weak against changing temperatures under different environment.

On the other hand, in ACF, only a fraction of the total bump areas is in electrical contact at each bump substrate metallization interconnection. It can be expected that the total current carrying capability is not as high as that of a solder joint. Therefore, ACF is suitable for the packaging of electronic device with low demand of I/O counts and current density.

1.4.4 Underfill Encapsulant

Underfill encapsulant is applied between the chip and substrate to protect the chip from environment effects and to compensate for the coefficient of thermal expansion (CTE) difference chip and substrate. The encapsulant should have low moisture absorption, and being a good barrier to mobile ions and flow properties. Furthermore, the encapsulant must have an excellent thermal conductivity to dissipate the heat generated by the IC and has a low curing temperature below the melting temperature of solder. Underfill encapsulant in use today is typically silica-filled epoxy based materials. In addition to tins, short fill and cure times are essential for cost saving and mass production. The underfill can be pre-applied onto the substrate before chip attachment or dispensed along two adjacent chip edges by capillary effect. The capillary action draws the underfill into the cavity between the chip and the substrate.

1.5 SOLDERING METHODS

1.5.1 Wave Soldering

Wave soldering is the most common soldering method for PTH assembly. The assembled PWB's are usually placed in a fixture, which carries the PWB's through the fluxer to apply an even and thin coat of flux on the underside of the board, and then the preheat stage to activate the flux. Finally, the board is passed through the molten solder bath, as shown in Figure 1.9. With the solder wave, the solder rises and forms solder joints by capillary effect. Sometime, an inert atmosphere of nitrogen (N_2) gas is used to improve the wetting properties, especially using Pb-free solders.

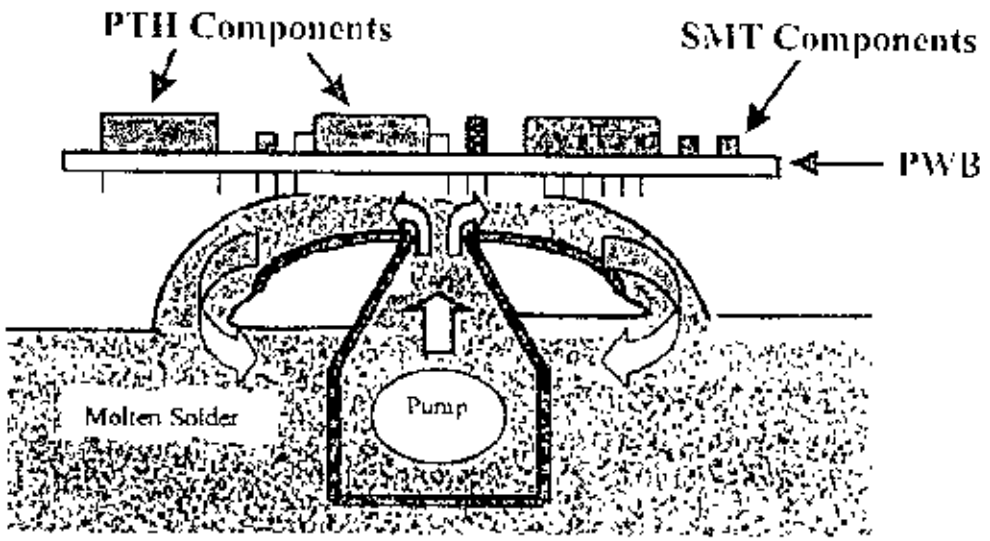

Figure 1.9 Wave soldering.

1.5.2 Reflow Soldering

Reflow soldering is a process, in which the solder paste is already placed on the solder pads before soldering begins. The increasing temperature in the reflow oven

activates the flux, and then re-melts solder paste to form solder joints. There are two types of reflow ovens, namely infrared (IR) and convection reflow ovens. In the IR reflow oven, the PWB's with components are directly heated by infrared radiation. Since the heat transfer is dependent on component color, size and nature on heat absorption, some radiation is reflected by the board and component surface. As a result, the heat distribution is not evenly on the board. On the other hand, heat transfer is accomplished by circulating hot gas in the convection oven. The oven temperature is more precisely defined and measurable than that in IR oven. Consequently, all the joints on the board reach the nearly same temperature to form the solder joints.

The reflow profile can be divided into four stages: (1) preheat, (2) thermal soak, (3) reflow, and (4) cool down, as shown in Figure 1.10. The reflow profile directly influences the manufacturing yield and the reliability of the assembly. The preheat stage is used to increase the temperature at a controlled rate to minimize any thermal damage to the components and board. Thermal soak is used to equalize the temperature of all surfaces being soldered and activated the flux to remove metal oxides. In the reflow stage, the solder reaches its melting temperature. The solder begins to wet the pad surfaces and the component leads to form intermetallic layer. The cool down stage allows the solder to solidify after reflow stage. It is essential to keep cool down stage under control. It is because the cooling rate will affect the microstructure of solder & subsequently affects the solder joint strength.

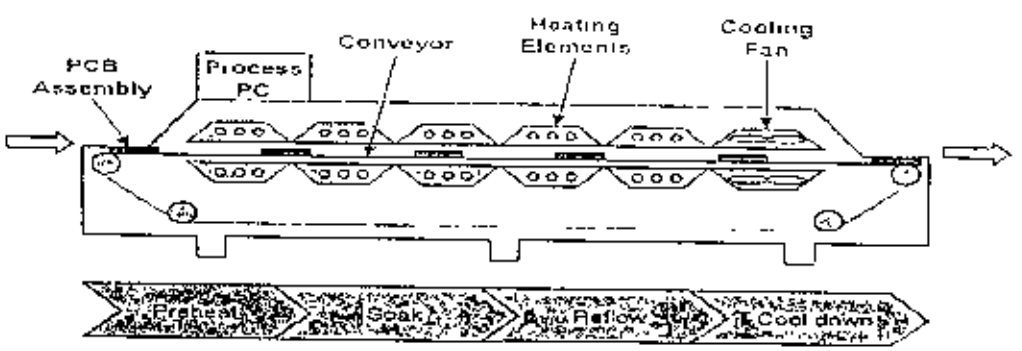

Figure 1.10 Reflow oven.

1.6 SCOPE OF STUDY

With the ever-increasing demand of electronic packaging, Sn-Pb solder plays an important role for interconnection materials. But, due to the ongoing concern regarding environmental pollutants, lead is being targeted in the electronic assembly arena. The study of lead-free solder has become a hot subject over the past few years. Government regulations are becoming stricter, and handlings of waste materials are becoming more regulated. Now is the time to take a serious look at alternative materials for making electrical interconnections. The history of government regulation suggests that targeted materials often become the subject of a ban within a certain timeframe; lead in paint, lead in plumbing, and lead in gasoline have all been eliminated thus far. There is no reason to believe that lead in solder will not meet the same fate. Thus it leads to the necessity to development of Pb-free solders. Even though many commercially available Pb-free solder alloys possess higher strength than the traditional Sn-Pb ones, there still exist reliability problems such as solderability and interfacial reaction on pad metallization. To develop new Pb-free solder Sn-9Zn has taken for this study. Here also some trace amount of Al & Cu added with the Sn-9Zn solder for better properties.

Pb hazards, environmental issues and some Pb-free binary alloys are introduced in Chapter 2. Alloying the raw materials to form solder alloys is shown in Chapter 3. After this, the effect of Al & Cu addition on microstructure of these alloys is investigated in Chapter 4. Since the mechanical properties are very dependent on the microstructure, tensile behavior and microhardness is studied in Chapter 5. Again the melting point is a vital character for any kind of solder, so DSC is carried out for these solder which also described in Chapter 5. Now-a-days composite approach is a very new technique to develop the properties of Pb-free solder. Thus, the composite effect of Ag micro particle in Sn-9Zn solder is discussed in Chapter 6. Finally, the overall conclusions are drawn from the entire study is precisely in Chapter 8 with some suggestions for further study.

CHAPTER 2

ENVIRONMENTAL ISSUES AND SOME Pb-FREE SOLDERS

2.1 ENVIRONMENTAL AND HEALTH PERSPECTIVES

In addition to technology advances, another strong driving force affecting the industry is the environmental and health/safety issue [7]. Within the electronic packaging and assembly industry, the top four issues related to global environment and public health are [7]:

- Ozone-depleting CFC elimination
- Wastewater handling
- Volatile Organic compound (VOC) control
- Pb control

Chlorofluorocarbons (CFCs) have been one of the most useful chemical groups serving several major industries effectively for many years. They are used as a coolant in refrigeration and air-conditioning, a foaming agent for plastic-foam metals, a propellant in aerosols, and a cleaning solvent for electronics and metal industry. Both government and industry have recognized the threat of ozone depletion and its relation to CFCs since the 1970s.

Wastewater from the cleaning step of the electronic packaging and assembly process needs attention for not only the environmental effect but also for economic reasons The concerns about contamination can be grouped into several areas [7]:

- pH
- Temperature
- Heavy metal
- Biological oxygen demand (BOD) and chemical oxygen demand (COD).

- Suspended solids
- Toxic chemicals or hazardous substances
- Pb content

The availability of a closed-loop water recycling system for a cleaning process makes in-process wastewater which needs disposal handling to a minimum. Most commercially available systems are capable of treating the bulk of in-process water for use as rinse supply and of removing waste removal without facing routine wastewater discharge problems.

Solder reaction is one of the oldest metallurgical processes for joining metal parts. Today, the use of solder in modern microelectronic technology is ubiquitous [8]. Traditionally, binary Sn–Pb solders are extensively used in electronic packaging. With the advent of area array packaging concepts (flip chip and ball grid arrays); usage of solders in die attachment is increasing sharply. The solder ball melts and forms a joint between the solder ball pad of the substrate and the ball itself. The performance of solder alloys has become one of the crucial roles in die attach application.

2.2 ENVIRONMENTAL AND HEALTH CONCERNS WITH LEAD

Pb has been used in electronic applications for more than 50 years. In the U.S., consumer electronics account for roughly 40% of the Pb found in landfills. As 315 million computers became obsolete between 1997 and 2004, nearly 1.2 billion lbs. of Pb potentially entered the waste stream [9]. Pb is a highly toxic metal, particularly dangerous when ingested by inhaling fumes (while melting, working with, or recycling it) or through drinking water. Fig. 2.1 schematically represents the path of Pb from electronic scrap to the human body through drinking water [10]. The following reactions are the mechanisms for Pb dissolution into water [11]. Pb becomes a water soluble compound by acidity rain.

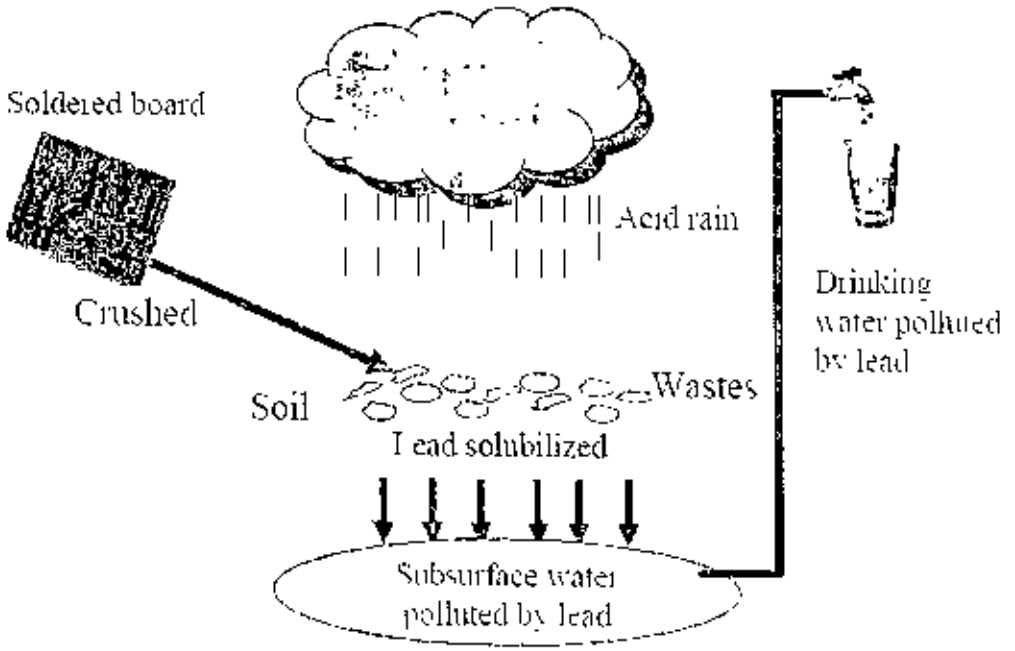

Figure 2.1 The path of Pb from soldered board to the human body via drinking water

$$Pb + 1/2\ O_2 \rightarrow PbO$$

$$Pb + H_2SO_4 \rightarrow PbSO_4 + H_2O$$

(acid rain)

$$PbO + 2HNO_3 \rightarrow Pb(NO_3)_2 + H_2O$$

(acid rain)

$$PbO + 2HCl \rightarrow PbCl_2 + H_2O$$

Table 2.1 Solubility of Pb compounds in water (g\l)

	10°C	20°C	30°C
$PbSO_4$	0.035	0.041	
$Pb(NO_3)_2$	483	565	1150
$PbCl_2$	6.7	9.9	26.2

When Pb accumulates in the body over time, it can have adverse health effects. Lead binds strongly to proteins in the body and inhibits normal processing and functions of the human body. Nervous and reproductive system disorders, delays in neurological and physical development, cognitive and behavioral changes, reduced production of hemoglobin resulting in anemia and hypertension [12] are some of the adverse effects of lead on human health. When the level of lead in the blood exceeds 50 mg/dl of blood, lead poisoning is considered to have occurred [13]. Recent studies have found that a Pb level even well below the established official threshold could be hazardous to a child's neurological and physical development.

Besides the environmental and toxic issues, Pb poses a radioactivity problem. Conventional Pb-containing solder contains a certain amount of radioactive Pb [14]. Since the radioactive Pb possesses a long half-life, it produces a particle during decay series, which frequently causes the failure of functional devices, particularly in memory chips [15-16]. This is often called soft errors in DRAM and charge-coupled devices (CCDs). For example, in a particle generates electron-hole pairs through elastic collisions during its penetration into Si. If the charge density in the capacitor of a memory cell changes, it results in a functional failure. Therefore, strict control of the amount of radioactive Pb or complete Pb removal is necessary especially for the application in high density memory chips.

2.3 LEGISLATION AND DIRECTIVES

Due to environmental and health issues, the usage of Pb-bearing solders have been eliminated in the electronic industry. It is because Pb or Pb-bearing compound, as cited by the Environmental Protection Agency (EPA) of the US, is one of the top 17 chemicals posing the greatest threat to human beings and environment [17]. Some corresponding law or directive are planned in European Union (EU), such as WEEE (Waste electrical and Electronic Equipment), which shall come into force at December 2008 and RoHS (Restriction of certain Hazardous Substances), which is effective since 1st July 2006 [18].

In addition, many companies have publicly announced their corporate policies on development and implementation of environmentally friendly technologies for a variety of reasons: to sustain resources, gain market-share, avoid trade barriers, or comply with potential legislation. In the electronic industry, the Pb generated by the disposal of electronic assemblies is considered as hazardous to the environment. In Japan, the legislation prohibiting Pb from being sent to landfills and other waste disposal sites is already in place. In the US, legislations in limiting the use of Pb have been introduced in both the Senate and the House of Representatives. The legislation includes (a) H. R. 2922, The Lead Based Paint Hazard Abatement Act of 1991, (b) S. 391, the Lead Exposure Reduction Act of 1991, and (c) H. R. 3554, the Lead Exposure Act of 1992 [19]. Although these bills have not been passed yet, it is likely that some form of bills will be passed in the future.

However, due to environmental and health concerns about the toxicity of lead, using of lead-containing solders for soldering in electronics is likely to be prohibited in the future. By fulfillment of related directives, many lead-free solder techniques are developed nowadays [20]. The lead-free solders have been developed so far in tin-rich binary and ternary alloy mainly. Binary alloys included Sn-Cu, Sn-Ag, Sn-Bi and Sn-Zn etc. Ternary alloys included Sn-Ag-Cu, Sn-Ag-Zn, etc.

2.4 THE ROLE OF Pb IN Sn-Pb SOLDERS

It is important to know the functions or properties Pb in the Sn-Pb solder. Firstly, Pb provides the ductility in the Sn-Pb solder [21]. Secondly, Pb lowers the surface tension of pure Sn from a value of 550mN/m at 232^{0}C to the value of 470mN/m at 280^{0}C for Sn- 37Pb [22]. Thirdly, Pb forms a eutectic alloy with the composition of 63wt%Sn- 37wt%Pb so that it has a low melting temperature at 183^{0}C in the Sn-Pb phase diagram as shown in Figure 2.3 [23]. Finally, Pb prevents the transformation of white or β-Sn phase (body-centered tetragonal structure) to gray or α-Sn phase (face-centered cubic structure), also referred as tin pest, upon cooling past 13^{0}C. This

transformation leads to 26% increase in volume and induce cracking in the Sn structure. Pure Sn is also prone to whisker growth. Sn whisker, β-Sn, is a single crystal growth in form of fine wire. Longer whiskers may cause shorts in PWBs. Pb is able to suppress whisker growth in Sn so that no whisker growth is encountered in Sn-Pb solder [19].

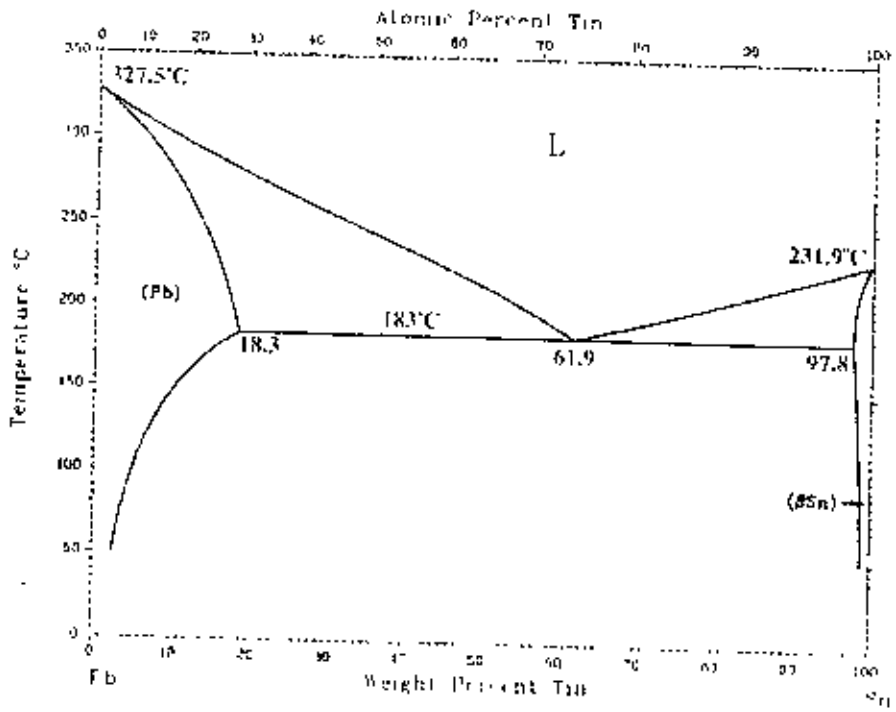

Figure 2.2 Pb-Sn phase diagram.

2.5 THE REQUIREMENTS FOR LEAD-FREE SOLDERS

Most Pb-free solders are Sn-based eutectic alloys of noble metals, such as Ag, Cu and Au. A eutectic alloy is used because it has a single and low melting point. Therefore, the entire solder joint will melt or solidify at eutectic temperature; otherwise, partial melting or solidification may occur. The main requirements for an alternative Pb-free solder alloy are:

- Low melting point: The melting point should be low enough to avoid thermal damage to the assembly being soldered, and high enough for the solder joint

composition should be determined by the needs of the performance level of a specific application [24].

Under severe operational environments, such as under-the-hood automobile applications, require the Pb-free solder joints with a superior performance and high reliability [25]. As a result, composite solders have been developed with enhanced strength and desired properties. Apart from the development of proper alloy compositions for the new solder systems, suitable fluxes and assembly process for Pb-free solders is also needed and considered [3].

All alternatives to the standard eutectic Sn-Pb solder investigated so far are based on Sn alloys with a Sn content significantly over 90 weight percent in combination with Cu, Ag, Sb, Bi or Zn. Among the binary alloys, Sn/0.5-0.8% Cu and Sn/3-4% Ag play a dominant role. Some possible binary solders are shown in table 2.1. The melting point of Sn-0.7%Cu is around 227^0C. The eutectic Sn-Ag solders exhibit melting points in the range of 220-221^{0}C, which is more than 30^0C above the melting point of the standard eutectic Sn-Pb solder. At present, near-eutectic Sn-Ag-Cu alloys are leading candidate solders. The ternary-eutectic composition is now thought to be close to Sn-3.5Ag-0.9Cu (wt.%), with a melting point of 217^0C. The Japan Electronics and Information Technology Industries Association (JEITA) recommended the Sn/3.0Ag/0.5Cu alloy [26]. The National Electronics Manufacturing Initiative (NEMI) Lead-free Assembly Project recommended the Sn/3.9Ag/0.6Cu (± 0.2 percent) alloy [27]. However, the high melting point of this alloy (217^0C) as compared to the traditional Sn-37Pb solders (183^0C) is still an issue in electronic packaging. Some other ternary alloys are shown Table 2.2.

Table 2.2 Some Possible Pb-free Binary Candidates

System	Known composition	Alloy price (US$/kg)	Melting temperature, ^{0}C	Remarks
Sn-Ag	96.5Sn/3.5Ag	13.90	221	Good thermal fatigue resistance
Sn-Sb	95Sn/5Sb	8.36	232-240	High melting point
Sn-Bi	58Bi/42Sn	7.79	138	Suitable for low temperature application
Sn-In	48Sn/52In	132.5	120	Expensive
Sn-Cu	99.3Sn/0.7Cu	7.66	227	Favorable price
Sn-Zn	91Sn/9Zn	7.99	199	Problem of oxidation, Strong dross formation

Table 2.3 Some Possible Pb-free Ternary Candidates

System	Known composition	Alloy price (US$/kg)	Melting temperature, ^{0}C	Remarks
Sn-Bi-Ag	Sn/4.8Bi/3.4Ag Sn/2Bi/3Ag Sn/6Bi/1.5Ag	13.72 13.17	211 203.6-231.1 187.6-228.9	Sn/Bi melts at 138^{0}C, obtained as a by-product of Pb extraction
Sn-Zn-In	Sn/9Zn/10In	51	178	Low melting point
Sn-In-Ag	Sn/20In/2.8Ag	58.1	138	Corrodes in combination with humidity, very soft, expansive
Sn-Ag-Cu	Sn/3.8Ag/0.7Cu Sn/3Ag/0.5Cu Sn/4Ag/0.5Cu	10.44 9.33 10.73	218.78 219.77 220.23	Good thermal fatigue properties at high temperature
Sn-Cu-Se (or Te)	95Sn/4.75Cu /0.25Se	53	210-217	Hardness, shear strength and % elongation are comparable with Sn-Ag-Cu

2.6 SOME WELL KNOWN LEAD-FREE SOLDER ALLOYS

2.6.1 Eutectic Sn-3.5Ag Alloy

The eutectic composition of Sn-Ag binary system is 96.5wt%Sn-3.5wt%Ag (Sn-3.5Ag) with melting temperature of 221^{0}C. The microstructure consists of β-Sn phase with dendritic structure and intermetallic Ag_3Sn in form of thin platelets. Intermetallic compound (IMC) is a compound of two metals that has a distinct chemical formula. In the Ag-Sn phase diagram as shown in Figure 2.4 [28], ϵ phase, Ag_3Sn, belongs to one kind of IMCs of Sn-Ag alloy and exists in a very narrow range of compositions. Because of the high concentration of Sn in this alloy, it may have Sn whisker growth.

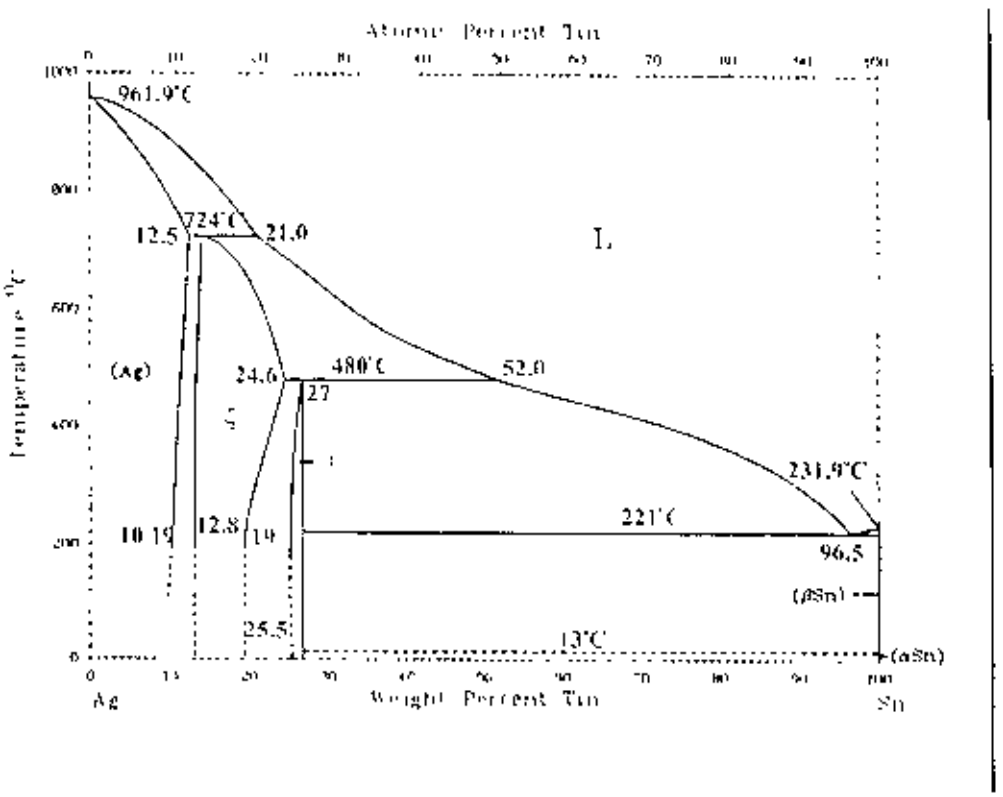

Figure 2.3 Ag-Sn phase diagram.

2.6.2 Eutectic Sn-0.7Cu Alloy

The Sn-Cu binary alloy has a eutectic composition of 99.3wt%Sn-0.7wt%Cu (Sn-0.7Cu) with melting temperature of 227^{0}C. The microstructure consists of β-Sn phase with dendritic structure and intermetallic Cu_6Sn_5 as hexagonal rods. In the Cu-Sn phase diagram as depicted in Figure 2.5 [29], two kinds of IMCs are commonly formed at the interface when the Pb-free solders are applied on Cu substrate. The η phase, Cu_6Sn_5, is always found inside the bulk solder as large facet and at the interface as IML in scalloped structure. The IML acts a metallic joining layer to provide the necessary bonding strength between the solder and the substrate. Another IMC, ϵ phase Cu_3Sn, usually appears between Cu_6Sn_5 and Cu substrate during thermal aging. The growth of these phases are reported to follow an Arrhenius relationship, with the activation energy for Cu_6Sn_5 being between 0.41 and 0.5 eV and for Cu_3Sn being between 1.06 and 1.27 eV, in the 90-170^{0}C range [30]. Similar to the Sn-3.5Ag solder alloy, this solder may favor to Sn whisker growth due to its high Sn composition.

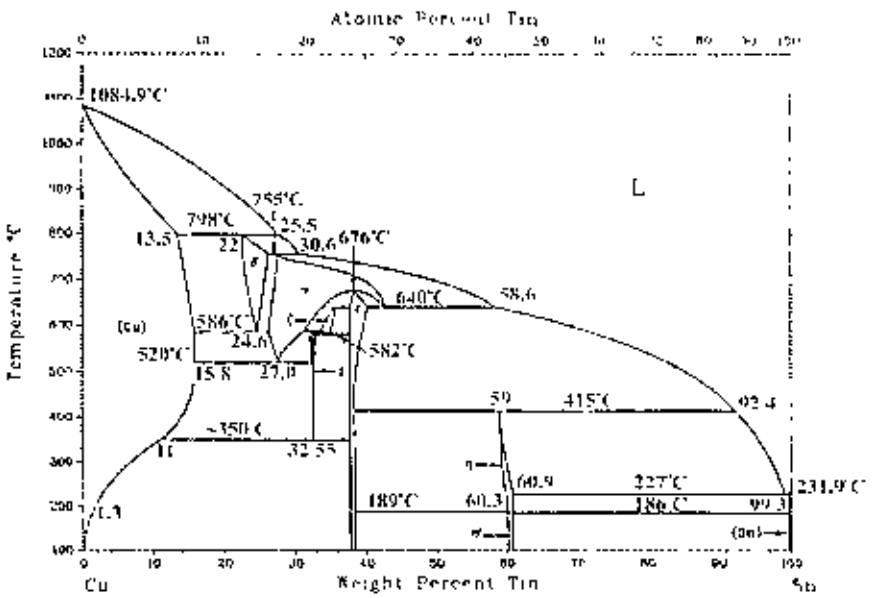

Figure 2.4 Cu-Sn phase diagram.

2.6.3 Eutectic Sn-52In Alloy

The eutectic composition of Sn-In binary system is 48.3wt%Sn-51.7wt%In (Sn-52In) with melting temperature of 120^{0}C. The eutectic microstructure consists of β-In, γ-Sn phase with dendritic structure and intermetallic In_3Sn in form of thin platelets. Intermetallic compound (IMC) is a compound of two metals that has a distinct chemical formula In the In-Sn phase diagram as shown in Figure 2.6 [31], β phase, In_3Sn, belongs to one kind of IMCs of Sn-In alloy and exists in a very wide range of compositions. Diffraction data show that In_3Sn (β) disproportionates to tetragonal (In) and hexagonal γ phase below about 140 K and reverses upon warming to room temperature. γ phase has been found at room temperature at the surface of solid β-phase samples [32]. Here less chance to Sn whisker growth due to presence of low Sn composition compared to Sn-3.5Ag and Sn-0.7Cu solder alloys.

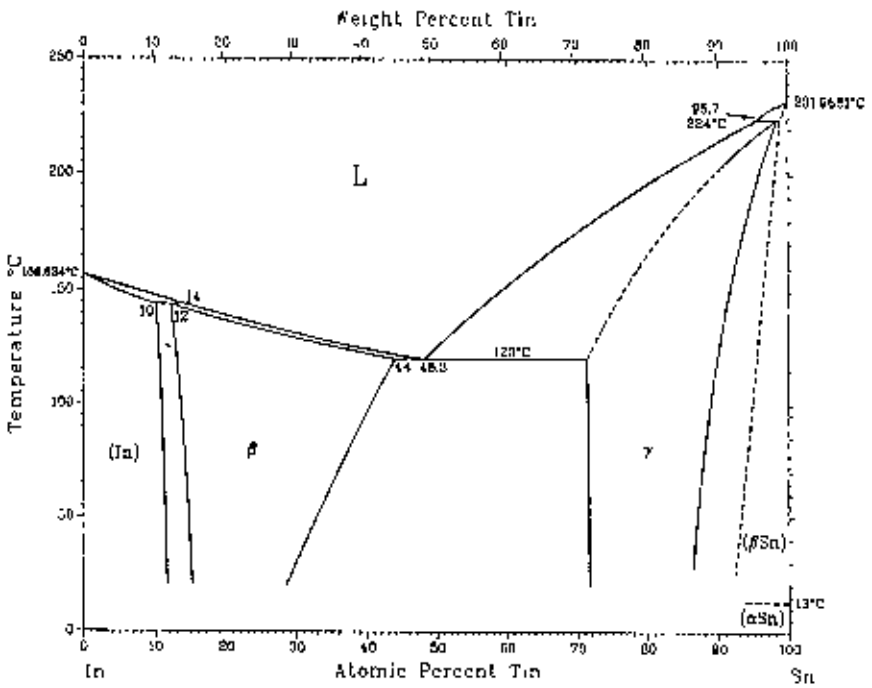

Figure 2.5 In-Sn phase diagram.

2.6.4 Eutectic Sn-9Zn alloy

The eutectic composition of Sn-Zn is 91wt%Sn-9wt%Zn (Sn-9Zn) with a melting temperature of 198^{0}C, as shown in Figure 2.7 [33]. Its eutectic microstructure consists of two phases: (1) a body-centered tetragonal β-Sn phase, and (2) a hexagonal Zn with less than 1wt% Sn in solid solution [34]. The microstructure can be expected to be lamellar, alternating of Sn-rich (β-Sn) and Zn-rich (Zn), under equilibrium solidification. Zn is very inexpensive and readily available. Also, Zn is extremely effective in reducing the melting point of Sn alloys. However, Zn reacts rapidly with oxygen. It forms excessive oxide or dross quickly during the wave soldering. More problematic is the very poor wetting properties due to the oxide formation. This technical problem can be overcome by using a special flux [35]. For this reason, Sn-Zn alloy is an attractive alternative to Pb-free solder.

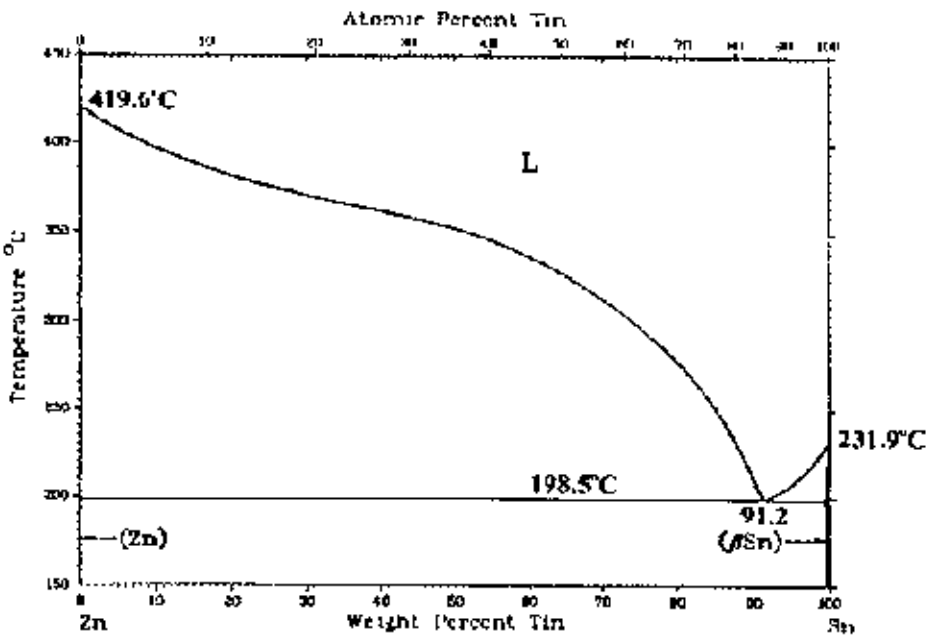

Figure 2.6 Sn-Zn phase diagram

2.7 COMPOSITE SOLDERS

2.7.1 What is Composite Solder?

Composite solders generally contain fine second-phase reinforcing particles dispersed uniformly in the solder matrix. i.e. solders with intentionally incorporated reinforcements are termed composite solders [36]. Composite approach was developed mainly to improve the service performance including service temperature capability. In other words, the basic purpose of this methodology is to engineer and stabilize a fine-grained microstructure, and homogenize solder joint deformation, so as to improve the mechanical properties of the solder joint, especially creep and thermo-mechanical fatigue resistance. An important additional feature is that the reinforcements do not alter the melting point of the solder matrix, but may effectively increase the service temperature of the base solder materials by improving the creep or thermo-mechanical fatigue properties of the solder matrix.

2.7.2 Important Considerations for Reinforcing Element

Reinforcements added to a solder matrix should satisfy certain conditions to enhance the service performance of the solder. Reinforcing phases should bond to the solder matrix, and the bonding can be weak or strong depending on the requirements for the specific application. Reinforcements must have minimal or no solubility in molten solder under normal reflow temperatures to maintain stability of the reinforcements during reflows. Reinforcements and the solder matrix densities should be closely matched to facilitate uniform distribution of the reinforcing phase throughout the matrix. If the densities are not matched, settling or floating of the reinforcements will cause the reinforcements to segregate within the solder, resulting in a non-uniform distribution [37]. Good wetting between the reinforcements and the solder matrix is also essential, since the interfacial strength could significantly alter the over-all mechanical behavior of the composite solder. The size of reinforcing phases should be optimal in order to stabilize the microstructure. It has been determined that reinforcement particles of size ~1μm or smaller tend to stabilize a very fine grained

microstructure [38, 39]. Reinforcement particles should not be prone to significant coarsening during reflow and service. Due to thermo-dynamic considerations, fine particles tend to coalesce to reduce the high interfacial energy associated with small particles.

Finally, reinforcements should neither significantly alter the processing temperature nor alter solderability (i.e., wetting characteristics of a solder with a chip carrier pad).

2.7.3 Purposes of Composite Solder

The methodology that will be employed to enhance the service performance of the solder joint should not affect the well laid out current metallurgical processes in the electronic manufacturing. It is essential that the incorporation of dispersoids does not significantly alter the solderability, solder/substrate wetting characteristics, melting temperature, etc.

Although one would prefer a strong solder joint for creep resistance considerations, it may not be ideal in electronic applications. If the solder in the joint is not able to dissipate the stresses that develop, failure of the electronic components will result. Therefore, a tradeoff is required between a strong solder joint to provide creep resistance but also one which is sufficiently compliant to dissipate stresses which could damage a device, that is, a solder joint must be capable of dissipating induced stresses, while still maintaining electrical functionality and mechanical integrity. Although these two requirements appear to be mutually exclusive, both of them can be satisfied by appropriate microstructural engineering of solders with suitable dispersoids.

2.7.4 Fabrication Techniques of Composite Solders

Usually, reinforcement particles used in the composite solder can be grouped into two categories. One kind of reinforcement addition involves the intermetallic particles. These intermetallic reinforcements can be incorporated to the solder matrix

either by adding preformed intermetallic particles (like Cu_6Sn_5, Cu_3Sn, or Ni_3Sn_4 [38, 40-45]) or by converting from elemental particles (like Cu, Ni, or Ag [40-2]) by their reaction with Sn during fabrication or the subsequent aging and reflow process. Another kind of reinforcement addition involves those having a low solubility and diffusivity in Sn, or even non-reactive with Sn. Examples of such reinforcements could be Fe particles [46] or oxide particles like Al_2O_3 or TiO_2 [39]. Choices of such reinforcements serve several purposes. Proper choice of foreign reinforcement additions could desirably introduce uniformly distributed intermetallic hard particles or non-coarsening particles. Well-dispersed reinforcements can serve as obstacles to grain growth, crack growth, and dislocation motion, so as to strengthen the solder against creep and fatigue deformation [38].

Two possible ways to introduce the desired reinforcements to the solder matrix are the in-situ method and the mechanical mixing method. In-situ method refers to the technique by which reinforcing phases, like Cu_6Sn_5 or Ni_3Sn_4 intermetallic particles, are readily formed upon processing the bulk solder itself [47-49].

The mechanical mixing method is more related to extrinsically adding reinforcement particles into the solder matrix, usually in the form of solder paste. The composite solder paste is usually prepared by mechanically blending the mixture for certain length of time to achieve uniform distribution of the reinforcements. After such significant mixing this mixture is melted to produce the composite solder. Traditionally, the reinforcement is usually added to the molten solder to produce the composite [40]. These reinforcements could be stable intermetallics or metallic particles that can form intermetallics during processing [37, 38, 41, 44, 50, 51]. The main aim of these approaches is to introduce compatible intermetallic reinforcements in the solder matrix. It is essential that these reinforcements do not significantly alter their size, shape and volume fraction during service.

2.7.5 Composite Approaches in Conventional Laded Solders

Dispersion strengthened in-situ composite solders of Sn-Pb-Ni and Sn-Pb-Cu alloys containing 0.1–1.0 μm dispersoids/reinforcements were produced by induction melting and inert gas atomization, by Sastry et al. [43]. It was found that, these composite solders showed an increase of 25–180% in yield stress and 20–80% in the modulus values compared to eutectic Sn-37Pb solder. Another type of dispersion strengthened composite solder was formulated by Betrabet et al. by adding 2.2 wt. % of Ni_3Sn_4 intermetallic particles into the Sn-40Pb solder matrix [38]. While Marshall et al. [42] improved the mechanical properties of conventional Sn40Pb solders by introducing Cu_6Sn_5 intermetallic compound (IMC) dispersoid. This investigation showed that ,the dispersion- strengthened solder had a finer grain size as the dispersoids acted as heterogeneous nucleation sites for the solder during solidification, leading to a 40% increase in fracture shear strain.

Mavooni and Jin prepared their composite solders by mixing 3 vol.% of 10 nm sized Al_2O_3 powders or 3 vol.% of 5 nm sized TiO_2 powders with 35 μm sized eutectic Sn-37 Pb solder powder [39]. Nano-sized, non-reacting, non-coarsening oxide particles formed uniform coatings of solder after repeated plastic deformation for rearrangement of the particles. Three orders decrease in the steady-state creep rate was achieved by this approach.

2.7.6 Composite Approaches in Lead-free Solders

In general, composite solders tend to render improved properties. The early reported investigations were basically exploratory in nature, and the extent of improvement must be weighed against environmental and economic factors before widespread adoption can be realized. However, studies on lead-free Sn-based composite solders have received attention only recently. Composite approaches used in lead-bearing solders can also be applied to lead-free solders. Although studies on composite solders utilizing lead-free solders are somewhat limited compared to those for solder

alloys themselves, development of lead-free composite solders is essential based on the reliability considerations.

Subramanian et al. have reported the microstructural evolution in the Cu_6Sn_5 particle reinforced eutectic Sn-3.5Ag based lead-free composite solders made by in-situ method [49]. While, Choi et al. reported the in-situ reinforcement of the same eutectic solder with Ni_3Sn_4 and $FeSn_2$ particles [52, 53]. Their investigation shows that intermetallic particles of Ni_3Sn_4 and $FeSn_2$ were found to be relatively stable even after 1,400 h of aging at 180^0C as compared to Cu_6Sn_5 intermetallic particles, an attribute desirable for a composite approach

The stability of mechanically-incorporated metallic reinforcement particles in the Sn-Ag composite solders was also examined after multiple reflows and during aging. The composite solders were prepared by mechanically blending nominally 15 vol.% of micron-sized Cu, Ag, or Ni particles with eutectic Sn-Ag solder to form a mixture with a uniform distribution of reinforcement particles [54, 55]. Since Ag particles consume less amount of Sn, thus change in composition of solder matrix was least in Ag reinforced composite solders compared to composite solders containing Cu and Ni reinforcements. Ag particles also exhibit higher resistance to coarsening than Cu and Ni reinforcement particles due to its lower diffusion coefficient in a Sn matrix.

Anderson *et al* [56] reported that the addition of 0.45wt% cobalt (Co) into Sn-3.6wt%Ag-1.0wt%Cu alloys refined the joint microstructure by enhancing nucleation of the Cu_6Sn_5 phase in the solder matrix. The Co also reduced intermetallic interface faceting and improved the ability of the solder joint samples to maintain their shear strength after aging for 72 hours at 150^0C. Recently, Kim *et. al* [57] investigated that the effect of the fourth elements, i.e., Fe, Ni, Co, Mn and Ti, on micro-structural features, under-cooling and tensile properties of Sn-3.0wt%Ag-0.5wt%Cu solder. They found that adding 0.1wt% of Ti, Ni, or Mn formed fine precipitates, consisting of Sn, Cu and additive, in the primary β-Sn grains and eutectic network band. Addition of Ti or Co provided the best under-cooling suppression. Also, Fe, Ti, and

Co increased 0.2% proof stress while they decreased elongation. In contrast, Mn and Ni improved ductility and also slightly improved 0.2% proof stress.

Cormack et al. have developed composite solders by adding 2.5 wt.% of ~2 μm magnetic Fe powders into pure Sn and eutectic Sn-Bi solder [46]. A fine, uniform dispersion of particles was obtained by imposing a magnetic field during the solidification process. The composite solder made by adding 2.5 wt.% of Fe powders to pure Sn exhibited 60~100% higher ultimate tensile strength than the dispersion-free solder materials. More importantly, its creep resistance at 100^0C showed an increase by a factor of 20. Fe particles reinforced eutectic Sn-Bi composite solder exhibited 10% higher tensile strength and five times improvement in creep resistance under similar conditions.

Zhong et al. recently reported the synthesis of high strength lead-free composite solder materials using nano Al_2O_3 as reinforcement [58]. Powder metallurgy was used to synthesize the Sn-based (91.4Sn-4In-4.1Ag-0.4Cu) composite solders containing different volume fractions of nano-sized alumina particulates. Results showed that the presence of nano Al_2O_3 particulates assisted in increasing both the 0.2%YS and UTS of the solder matrix all extrusion temperatures employed.

2.8 SELECTION OF LEAD-FREE SOLDER

Starting with the above list, we began to search for the best alloy, the choices of acceptable elements dwindles rapidly. Silver is in adequate supply but has a cost disadvantage. Bismuth poses a potential supply problem since it is a by-product of lead mining, and also has embrittlement problems. Bismuth is also a poor conductor, both thermally and electrically. Concerning cadmium, toxicity is the leading reason not to use this element. With copper, there is plenty of supply, and it is soluble in tin. In low percentages, copper works well. There is a long history of tin alloys containing copper. Gallium supply and costs are the main reason not to use it, as well as its brittleness. The cost, inadequate supply, poor resistance to corrosion and rapid oxide formation during melting all eliminate the element indium.

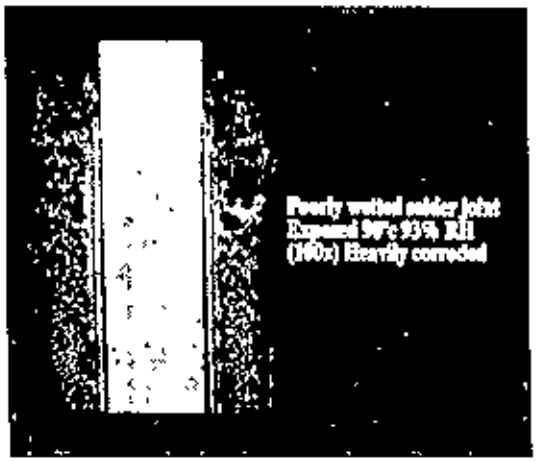

$4In + 3O_2 \rightarrow 2In_2O_3$

$2In_2O_3 + 12HCl \rightarrow 4InCl_3 + 6H_2O$

$4InCl_3 + 6H_2O + 6CO_2 \rightarrow 2In_2(CO_3)_3 + 12HCl$

$2In_2(CO_3)_3 + 6H_2O \rightarrow 6CO_2 + 4In(OH)_3$

Net reaction: $4In + 3O_2 + 6H_2O \rightarrow 4In(OH)_3$

Figure 2.7 Corrosion of Sn-In eutectic solder and corrosion reaction of Indium

Figure 2.8 shows a solder fillet formed with an indium eutectic, aged at 90°C and 93% relative humidity. The corrosion of indium can be seen as the dark areas on the solder joint. The remaining area is the tin. The reaction that has occurred is also seen in figure 2.8. For the most part, indium is safe if kept in low humidity conditions, or if it is conformally coated. Antimony has an adequate history and supply to be a viable solder additive. Tin is the base of solders, toxicity is low and supply is adequate. Zinc is in adequate supply, but has oxidation problems and also causes solder to become brittle. This oxidation problem creates an issue with existing automatic soldering equipment [59]

Among all these Sn–Zn eutectic system is one of the most promising lead-free solders with the advantages of low melting points, excellent mechanical properties and acceptable costs; whereas it's poor wetting ability confines its applications in many substrates, which can be improved by some third particle addition [60].

CHAPTER 3

DEVELOPMENT OF NEW Pb-FREE SOLDER ALLOYS

3.1 INTRODUCTION

In order to develop new Pb-free solder alloys with better performance and reliability, trace amount of Al and Cu were doped with binary eutectic Sn-9Zn solder. Generally speaking, both Sn-9Zn-Al and Sn-9Zn-Cu alloys are the composite solder because the Al reacts with both Sn or Zn and form IMC which dispersed in the eutectic solder matrix. Also, the addition of Al has a grain refinement affect on the microstructure by restraining the sizes of the β-Sn phase and the IMCs. On the other hand, Cu forms Cu_5Zn_8 IMC in the bulk eutectic Sn-9Zn solder which depletes the whole solder alloy from Zn rich phase resulting lack of strength in the bulk solder. This will be discussed in the following chapter.

3.1.1 Role of Al and Cu on Sn-9Zn Eutectic Pb-Free Solder

As reported by S. Vaynman et al. [61] Sn-9Zn eutectic solders have limited commercial viability due to its serious oxidation and wetting problems. Addition of alloying elements is an effective way to improve oxidation resistance and wetting behavior of eutectic Sn-9Zn solder alloy.

Al can improve the oxidation resistance of Sn-Zn alloy. According to Chen et al. [62], the additions of Al can form an oxidation film, which is relatively stable and compact, preferentially to the Zn on the solder surface. This oxidation film also prevents solder from further oxidation. As a stable and compact oxide, Al_2O_3 is difficult to remove by soldering flux, and as well as this oxidation film is detrimental to the wetting properties of Sn-9Zn solder.

Small alloying additions have limited effects on the melting point of Sn-9Zn solder. From the SEM micrographs it had been found that the addition of small quantities of alloying elements do not cause great changes in the microstructure or thermal properties of Sn-9Zn solder [62].

Addition of Al significantly improves the plasticity of the Sn-9Zn solder while maintaining its tensile strength. It is presumed that addition of Al destroys the coarse and brittle Zn-rich phase and forms a much finer microstructure, which benefits plasticity and results in an improvement on the tensile strength [62]. C. M. Chuang et al [63] reported that the deterioration of the tensile properties of Sn-9Zn and Sn-9Zn-0.5Al specimens corresponded to the number of days of naturally aging. Al has been incorporated with Zn to enhance the atmospheric corrosion resistance of the conventional galvanizing coatings for steel. Zn-5Al and 55Al-Zn coatings are the most commonly commercialized Al-Zn series of coatings such as GALFAN® and GALVALUME®. A series of studies also tried to incorporate Al with the Sn-Zn solders. The addition of Al to the Sn-Zn solder is kept at low levels in order to keep the melting point as low as possible. An equilibrium phase diagram has been reported for this particular ternary system which has a eutectic point at 197^0C. The ternary Sn-Zn-Al system possesses a complicated phase transition behavior based on the equilibrium studies mentioned above [64].

The solders may encounter a solidification sequence during the fabrication of the electronic interconnections, for instance, the wave soldering or solder reflow. A detailed understanding of the solidification behavior as well as the phase formation is of interest as far as the control of the solder joint property is concerned [65].

The addition of Cu can increase the melting point of solder alloy, as Cu has far higher melting point than that of Sn-9Zn solder alloy, thus increasing the alloy melting process. The Sn-Zn-Cu (SZC) solder had a near eutectic reaction in 214.93^0C [66]. By using midely active rosin (RMA) flux, the wetting angle of Sn-9Zn was found to be 89^0, and with addition of 4% Cu with 0.05% of rare earth, the alloy

wetting angle was found to be minimum 49^0[67]. It had been proven that by alloying Cu with Sn-Zn-Al the melting temperature increases about 210^0C. Cu has the ability to stabilize Zn in the solder and controls the growth of the reaction layer [68]. With the addition of Cu in the Sn-Zn alloy, the Cu-Zn compound formed in the solder matrix prevent the Zn atoms to diffuse in the Cu foil, which causes the planar rod-shape Cu_5Zn_8 IMC at the interface change into scallop Cu_6Sn_5 IMC. It was observed that the IMC of Sn-Zn-xCu/Cu joint is mainly Cu_5Zn_8 when the content of Cu is 0-1%; when the content of Cu is 2%-6%, the IMC is Cu_6Sn_5 and Cu_5Zn_8 together; when the content of Cu is 8%, the IMC is Cu_6Sn_5. With the increasing of Cu in the Sn-Zn-xCu solder, the shear strength of the Sn-Zn-xCu/Cu solder joint is enhanced with the transformation of IMC type from planar Cu_5Zn_8 to scallop Cu_6Sn_5 at the interface [69].

3.2 THE MANUFACTURE OF Pb-FREE SOLDER ALLOYS

3.2.1 Raw Materials

The Pb-free alloys were prepared from commercially pure Sn ingot (99.39%), Zn (99.99%), Al (99.99%) and Cu (99.99%).

3.2.2 Ingot Preparation

The elemental ingots are placed into a pit furnace under controlled atmosphere according to the binary eutectic composition to prepare the master alloy. They were melted in a pit furnace at a temperature of 500^0C. Then the molten metal was chill cast in a steel mold. The ingots of Sn-9Zn-0.5Al and Sn-9Zn-0.7Cu were also prepared following the same procedure. For Sn-9Zn-0.5Al and Sn-9Zn-0.2Cu alloy preparation the furnace temperature was kept at 500^0C for some time to homogenize the structure and also to enhance Al and Cu dissolution in the solder matrix. Consequently, wet chemical analyses were done to determine the exact composition

of the casting ingots and also with the energy dispersive x-ray (EDX) analysis. The chemical compositions of the alloys are listed in Table 1.

Table 3.1 Chemical composition of starting materials (wt. %)

Alloys	Sn	Zn	Al	Cu	Pb	Sb	Bi
Sn Ingot	Bal.	-	-	-	0.346	0.253	0.009
Sn-9Zn	Bal.	8.683	-	-	0.343	0.251	0.012
Sn-9Zn-0.5Al	Bal.	8.601	0.520	-	0.346	0.252	0.010
Sn-9Zn-0.7Cu	Bal.	8.626	-	0.682	0.340	0.260	0.008

These chill-cast ingots were used for following purposes.

1. Cut small pieces for microstructure examination and also for micro-hardness test.
2. Collect very small sample of 10-20 mg to conduct DSC.
3. Prepare tensile specimens by mechanical machining.

CHAPTER 4

EFFECT OF ADDITION OF A THIRD ELEMENT ON MICROSTRUCTURE OF Sn-9Zn Pb-FREE ALLOY

4.1 INTRODUCTION

The chilled-cast ingots are used to study the microstructure of the Pb-free solders. The ingots were cut and mounted in resin, cured at room temperature, mechanically ground with sand papers. After that, each sample was polished with 0.5μm Al_2O_3 particles in order to obtain the microstructure. After cleaning with acetone and alcohol, the sample was investigated by optical microscope (OM) and followed by scanning electron microscope (SEM). Also, energy dispersive x-ray (EDX) analysis was used to determine the elemental compositions at selected spots and areas. The chemical analyses of the EDX spectra were corrected by standard ZAF software. The backscattered electron imaging mode of the SEM was used to study the microstructure.

4.2 MICROSTRUCTURE OF Sn-9Zn LEAD-FREE ALLOYS

Figure 4.1a shows the microstructure of a pure as cast Sn under OM examination. As it is pure tin, thus only plain single Sn phase is observed from the micrograph. Figure 4.1b shows the microstructure of the eutectic Sn-9Zn. It has been mentioned that the eutectic Sn-9Zn alloy consists of β-Sn and Zn-rich phases. In the micrograph, the bright regions are the β-Sn phase and the dark region between the β-Sn grains is the Zn-rich phase. With the addition of 0.5% Al in the eutectic Sn-9Zn, the Zn-rich phase

decreases drastically and also become finer than before. As Zn is a very reactive material (electro negativity: -1.65), it forms compound with the aluminum (Al).

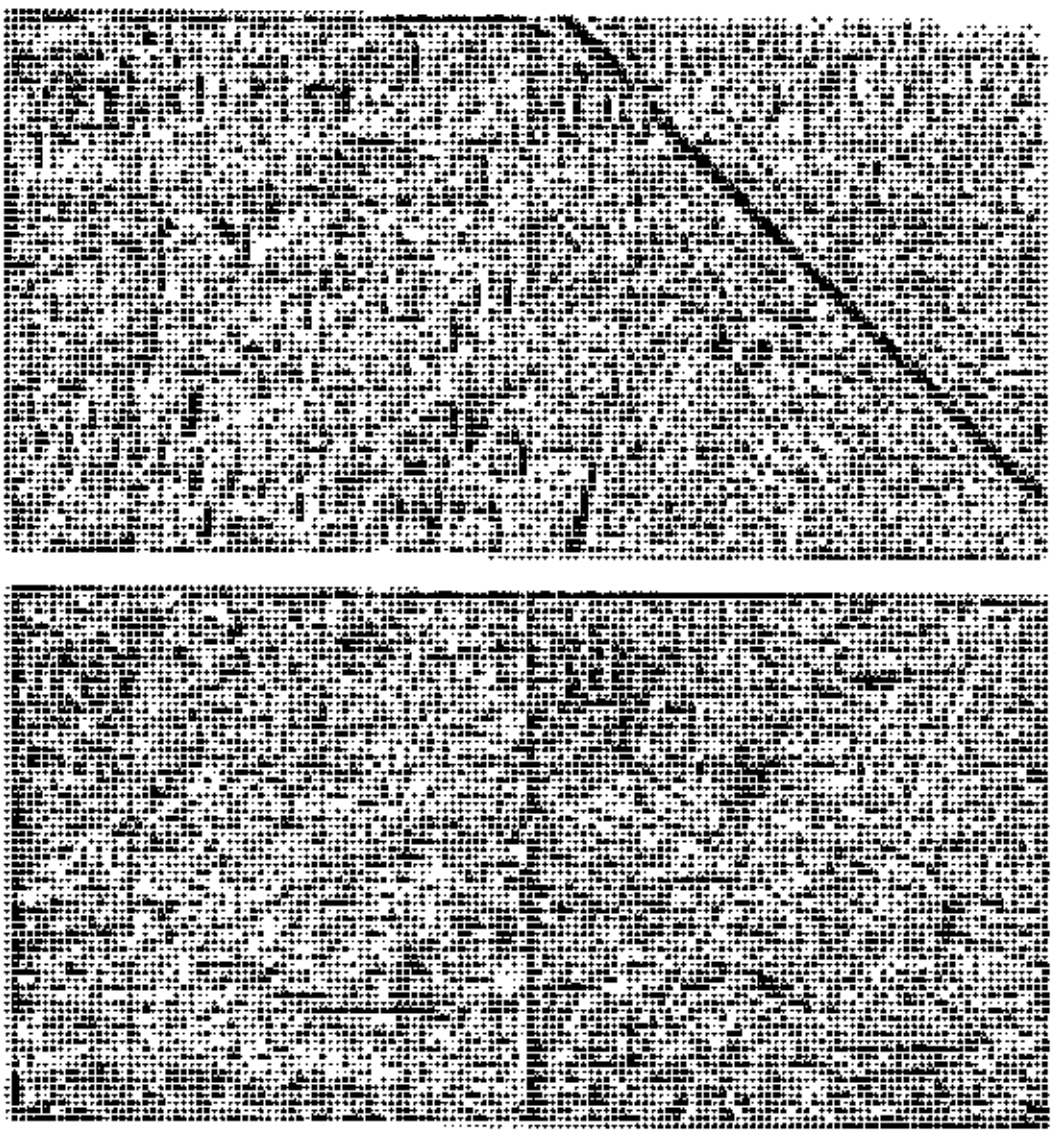

Figure 4.1 Optical micrographs of the chill-cast samples of (a) Pure Sn, (b) Sn-9Zn, (c) Sn-9Zn-0.5Al, and (d) Sn-9Zn-0.7Cu (all images taken at 200X).

The compounds of Zn-Al-Sn are dispersed in the whole matrix. Figure 4.1c shows the microstructure of the Sn-9Zn-0.5Al observed under OM. Again with the addition

of 0.7% Cu with the eutectic Sn-9Zn, the coarse α-Zn phases became smaller, as shown in Figure 4.1d.

The microstructures of Sn-9Zn and Sn-9Zn-X alloys are also examined under SEM in the Back Scattered Electron (BSE) mode, as displayed in Figure 4.2 a-d. Figure 4.2a shows the microstructure of pure chill-cast Sn, which contains only single Sn phase and some pores in it. Figure 4.2b shows the typical lamella of eutectic microstructure. The primarily solidified phase, the dark phase of Sn-9Zn microstructure consists of fine needlelike Zn-rich phase in β-Sn matrix. Also some Zinc spheroids are observed in the microstructure. With the addition of 0.5% Al, the eutectic Sn-9Zn alloy shows small precipitates distributed in the eutectic phase When 0.7% Cu is added with the eutectic Sn-9Zn alloy, the microstructure changes with some planar and flower shaped intermetallic compound distributed in the typical eutectic lamella as shown in Figure 4.2d. For both cases when a third element (Al or Cu) added with the Sn-9Zn eutectic alloy, the α-Zn phases decreased and changes to finer structure. Also it reacts with the third element and form intermetallic compounds due to its very reactive nature. And due to the high reactivity of Cu, the microstructure of Sn-9Zn-0.7Cu deprived of thick Zn-rich eutectic lamella and consists of fine eutectic colonies dispersed with both Sn-Cu and Zn-Cu IMCs.

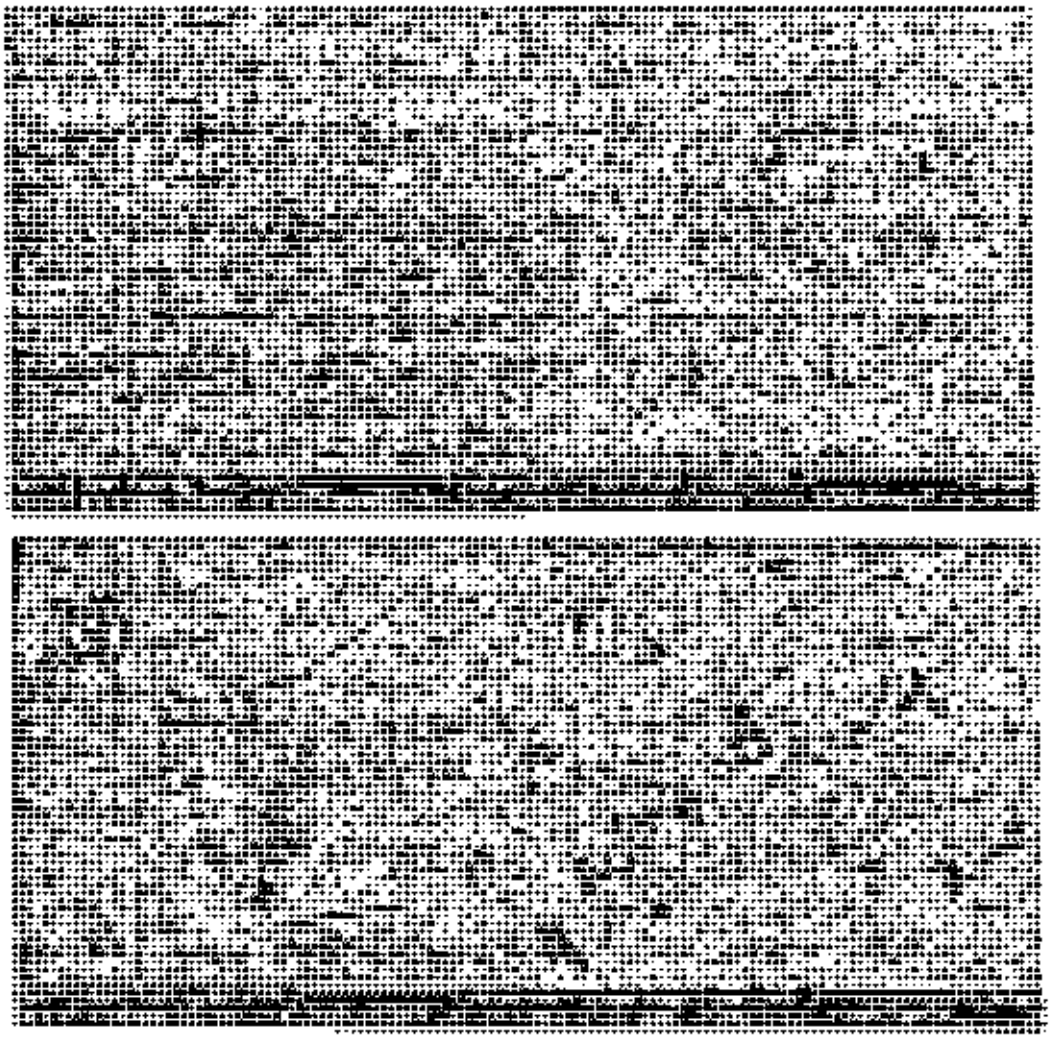

Figure 4.2 SEM microstructure of chill-cast samples of (a) Pure Sn, (b) Sn-9Zn, (c) Sn-9Zn-0.5Al, and (d) Sn-9Zn-0.7Cu (all images taken at 500X).

It is clear from the above discussion that a third element effectively changes the microstructure of eutectic Sn-9Zn solder alloy In order to analyze the distribution of different elements in different phases and IMCs. EDX analysis is used to determine the elemental composition at selected areas and spots of Sn-9Zn-X alloy. Figure 4.3 shows the microstructure of a pure tin with EDX spectrum analysis.

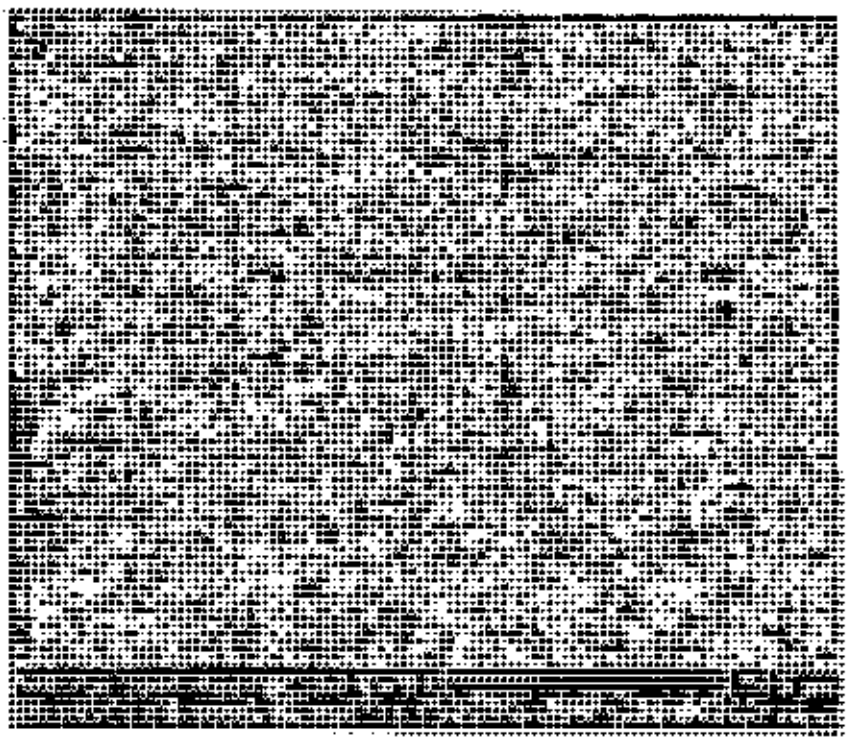

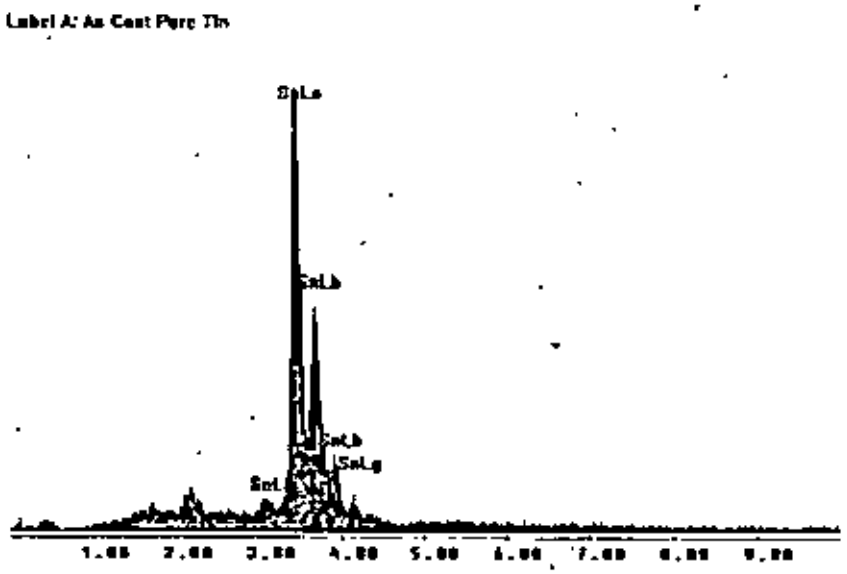

Figure 4.3 SEM microstructure of chill-cast pure Sn with EDX spectrum.

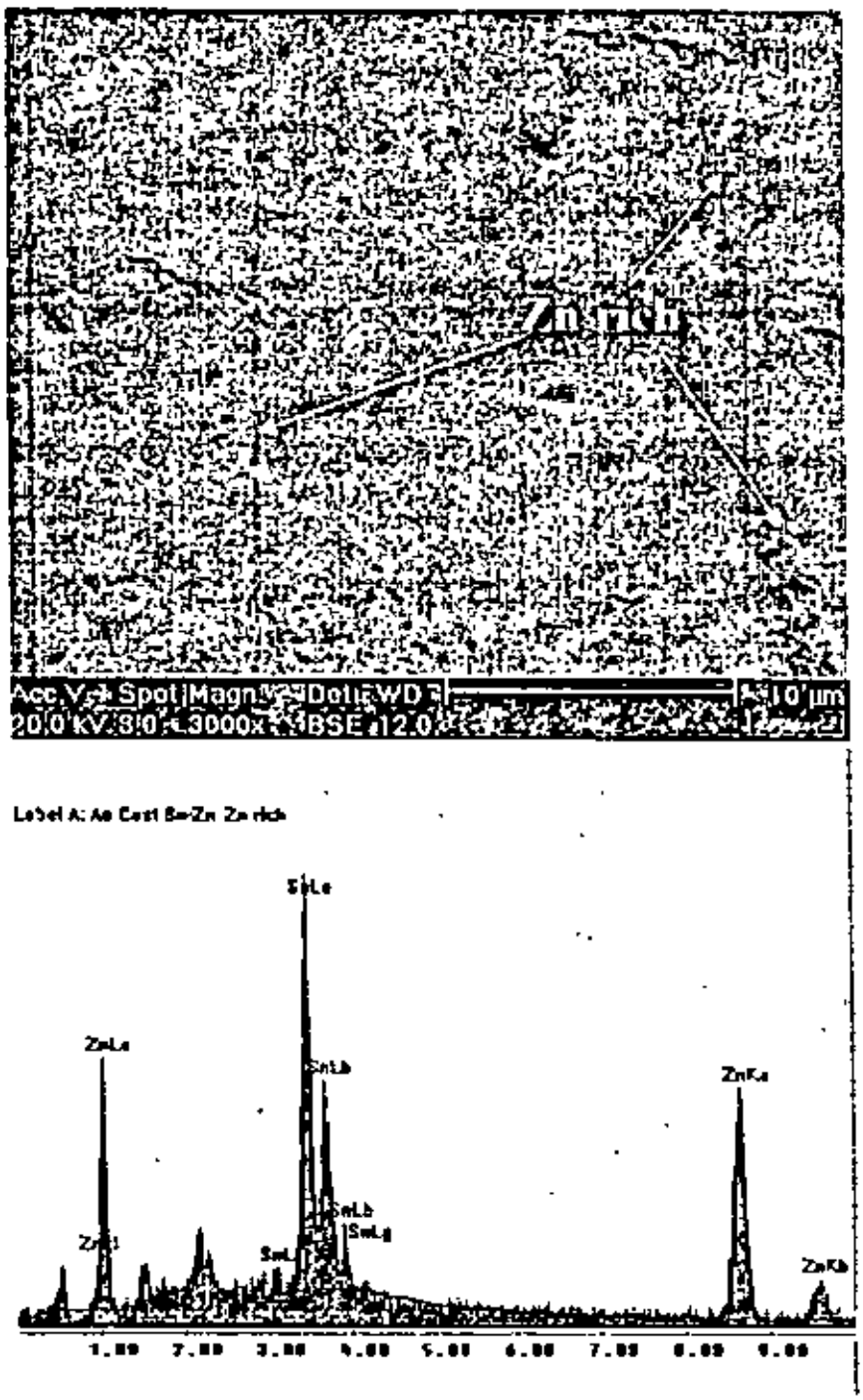

Figure 4.4 SEM microstructure of chill-cast eutectic Sn-9Zn with EDX spectrum of α-Zn phase.

In Figure 4.4, the platelet-shaped Zn-rich phase is discretely dispersed in the β-Sn matrix. The EDX result shows that small amount of Sn present in the Zn-rich phase, while no Zn is detected from the β-Sn matrix.

Figure 4.5 shows small precipitates distributed in the eutectic phase. The primarily solidified phase, the dark phase in Figure 4.5, of the eutectic structure was analyzed and consists of Sn, Zn and Al, while the composition of the secondarily solidified phase, the white phase of Figure 4.5, was β-Sn phase. This is reasonable as the phase with greater contents of Al and Zn is expected to solidify first.

The composition, analyzed with EDX, of this small precipitates, Fig. 4.5, is (42.16~49.25)Al-(19.22~20.34)Zn-(37.5~43.06)Sn, corresponding to the stoichioeatry of Al_6Zn_3Sn. The high Al and Zn contents of this precipitate are indicative that it precipitates prior to the eutectic reaction.

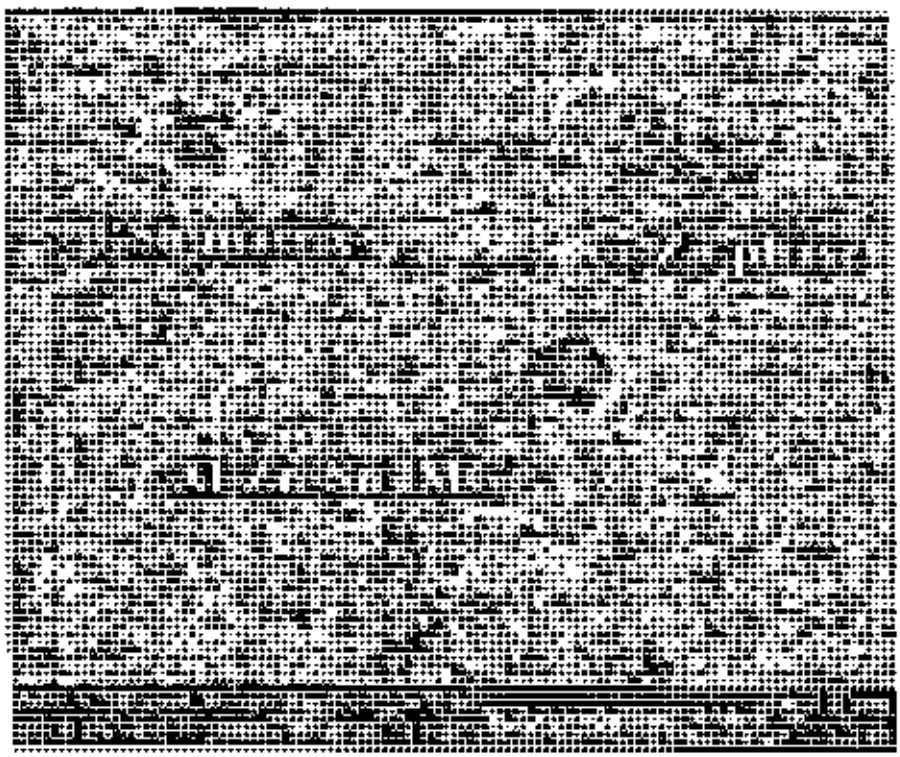

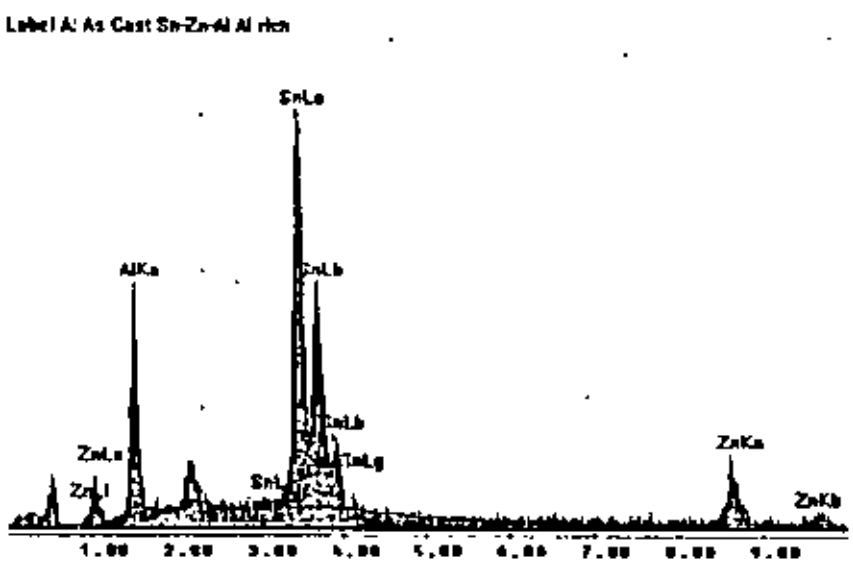

Figure 4.5 SEM microstructure of chill-cast Sn-9Zn-0.5Al with EDX spectrum of small IMC of Al-Zn-Sn.

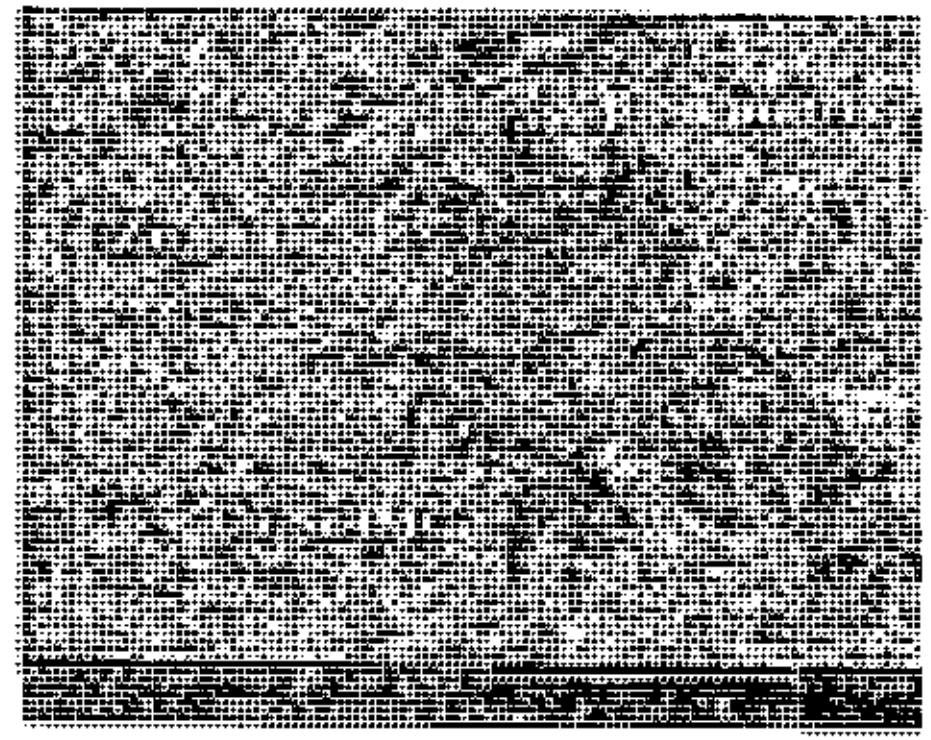

Label A: As Cast Sn-Zn-Cu Cu-Sn rich

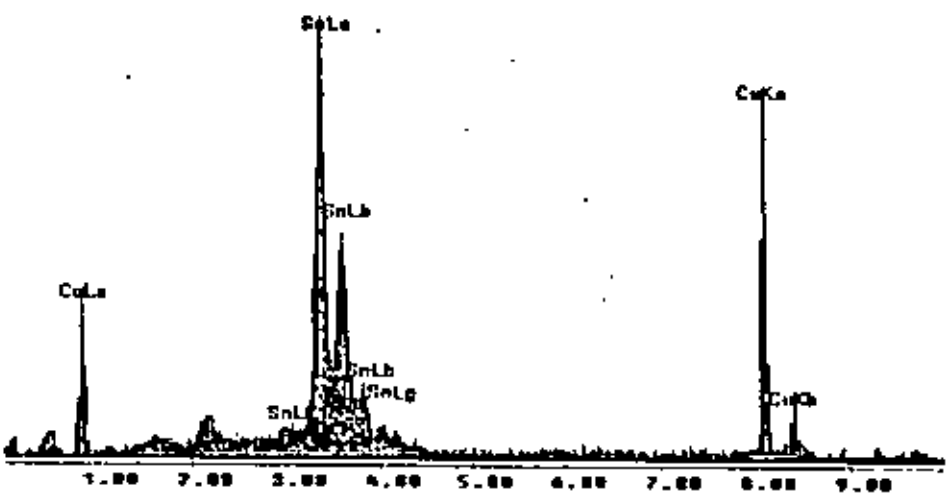

Figure 4.6 SEM microstructure of chill-cast Sn-9Zn-0.7Cu with EDX spectrum of Cu-Sn rich phase.

Label A: As Cast Sn-Zn-Cu Cu-Zn rich

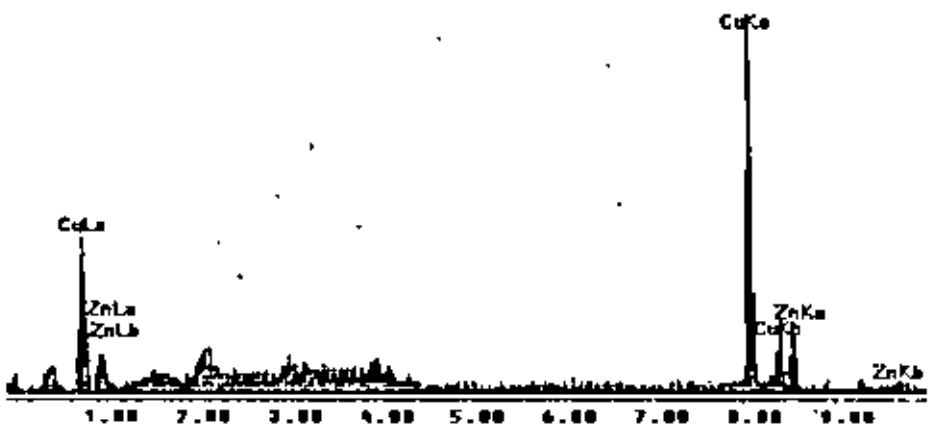

Figure 4.7 SEM microstructure of chill-cast Sn-9Zn-0.7Cu with EDX spectrum of Cu-Zn rich phase.

Figure 4.6 shows "flower shaped" precipitates in the eutectic Sn-Zn phase, where figure 4.7 shows planar shaped IMC in the Sn-Zn matrix. Now it is clear that the Sn-

9Zn-0.7Cu alloy was consist of four different phases: β-Sn matrix, α-Zn phase with some flower shaped Cu_6Sn_5 and planar shaped Cu_5Zn_8 IMCs. The composition, analyzed with EDX, of these flower shaped precipitate (Fig. 4.6) is (38.62~43.33)Cu and (59.13~63.54)Sn, corresponding to the stoichioeatry of Cu_6Sn_5, whereas the planar shaped precipitate (Fig. 4.7) is (42.16~49.25)Cu and (19.22~20.34)Zn, corresponding to the stoichioeatry of Cu_5Zn_8. The high Cu content of these precipitates are also indicative that these IMCs precipitate prior to the eutectic reaction.

Based on OM and SEM micrographs, the addition of Al and Cu in Sn-9Zn alloy is able to restrain the β-Sn phase and eutectic lamella. Also, the small platelets of Zn-rich phase are uniformly distributed in the β-Sn matrix. For the Sn-9Zn-X alloy, the finer α-Zn phase and the new IMCs are observed in the β-Sn matrix.

4.3 CONCLUSIONS

With the addition of the Al and Cu, the microstructures of eutectic Sn-9Zn Pb-free solders become more uniform than their respective microstructures without the addition of these elements. The size of eutectic lamella is decreased and the Al_6Zn_3Sn, Cu_6Sn_5 and Cu_5Zn_8 IMCs formed in the eutectic colonies, when Al and Cu are added in Sn-9Zn alloy respectively. Both Sn-rich and Zn-rich phase are also reduced in size after the addition of Al and Cu. The reason of uniform microstructure obtained by the addition of a third element is that these elements form IMCs in the molten solder and promote a high nucleation density of the second phase in the eutectic colony during solidification.

CHAPTER 5

MECHANICAL PROPERTIES OF Pb-FREE SOLDER ALLOYS

5.1 INTRODUCTION

Modern electronic assemblies are made up from materials with a wide range of thermal expansion coefficients. When an electronic device is in operation, it normally generates heat. As these materials are packaged together in the device, internal thermal stresses and strains will result under temperature excursions during operation. This is why one of the main focuses in material selection for electronic assembly is to provide the least amount of thermal mismatch. However, in practice, this cannot be fully achieved and the thermal stresses in an assembly are unavoidable. It is therefore important for solder alloys, as prime interconnection materials, to be able to withstand the high thermal stresses. It is also known that the absolute operating temperature, T_{op}, is very close to absolute melting temperature, T_m, of the solder. As a result, the homologous temperature, ($\eta=T_{op}/T_m$), is usually greater than 0.6 when the assembly is operated at room temperature. Hence, the solder material is normally subjected to creep during operation even at room temperature. This means that the Pb-free solders should have their melting point low enough to be comparable with that of Sn-37Pb and as well as high enough for the solder joint to bear the operating temperatures. Besides, the Pb-free solders should have and retain adequate mechanical strength such as tensile and creep resistance during their operation. As the mechanical strength and melting behavior of solder alloys are important for a successful solder alloy, this chapter discusses mainly these issues

5.2 MELTING BEHAVIOR

Soldering, a joining process of two substrates, is a very important technique in the packaging of electronic products. As per the temperature profile of the reflow furnace, the solders are first heated up, then become molten, react with the substrates; cool down, and lastly solidify. The temperature profile of the reflow furnace is the key process controller for obtaining a good assembly. Insufficient heating can result in non-wetting at the solder joint, whereas excessive heating introduces enhanced interfacial reactions and possible reliability problems [70]. The knowledge of melting and solidification characteristics of solders is crucial in the selection of the temperature profile for the reflow furnace.

A differential scanning calorimeter (DSC Q-10) is used in the present study to determine the melting and solidification characteristics, such as the onset temperatures of phase transformation and the enthalpy of fusion of the different Pb-free alloys. The heating rate for the DSC test is 10^0C/min in nitrogen atmosphere. The temperature range was from 30^0C to 250^0C during the analyses. The first onset temperature is the temperature at which the sample begins to melt, and is regarded as the solidus line [71]. The peak temperature occurs at the end of melting range of sample, and is regarded as the liquidus line. So the DSC can be used to find the melting temperature and as well as the melting range of Pb-free solder alloy.

5.2.1 Melting Temperature of Sn-9Zn-X Alloy

Figure 5.1a shows the DSC curve for the Sn and the melting temperature was found at 229.23^0C. Figure 5.1b shows the DSC curve for the eutectic Sn-9Zn alloy and here the melting temperature was observed at 197.59^0C.

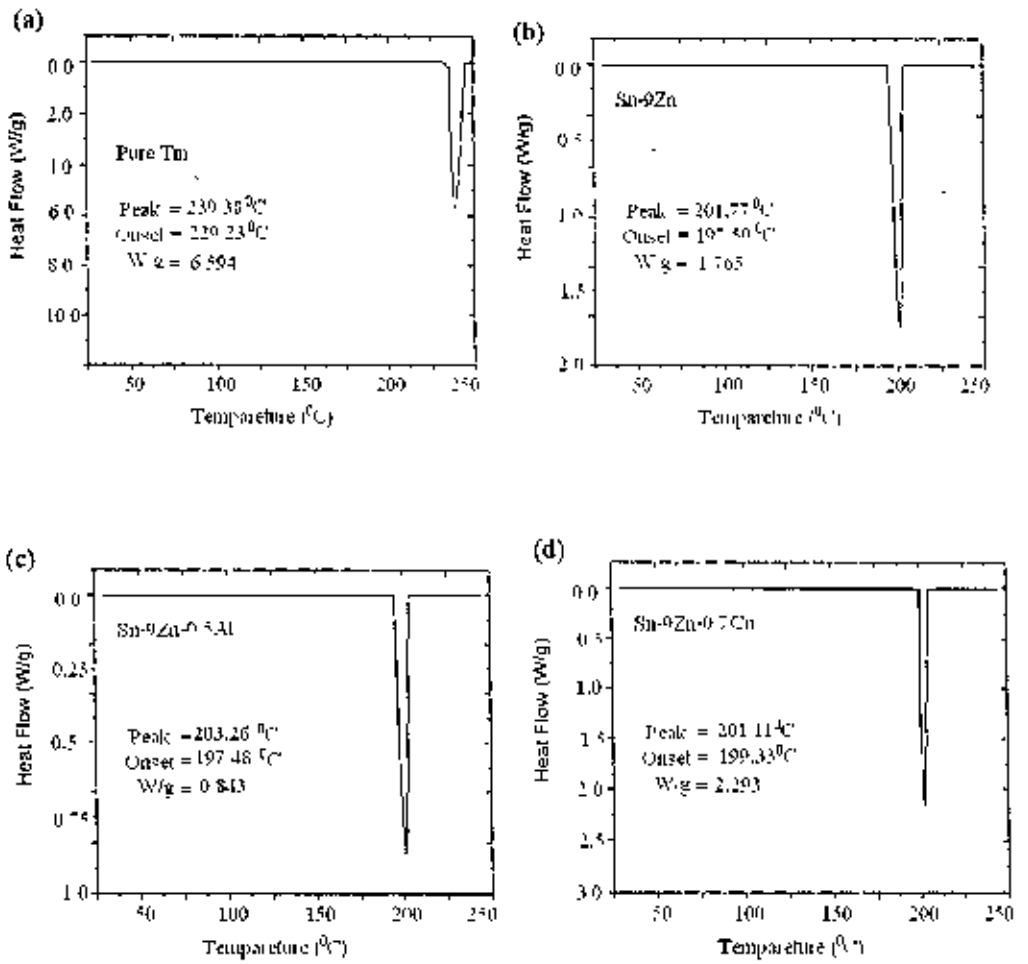

Figure 5.1 The DSC curves on heating (a) Pure Sn, (b) Sn-9Zn, (c) Sn-9Zn-0.5Al, and (d) Sn-9Zn-0.7Cu.

With the addition of 0.5% Al the melting temperature changes only slightly. As illustrated in the Figure 5.1c, the melting temperature is 197.48^{0}C for Sn-9Zn-0.5Al. It indicates that the addition of small amount of Al into Sn-9Zn alloy does not cause significant increase of the melting temperature. But, when small amount of Cu is added to the Sn-9Zn eutectic solder alloy, the melting temperature increases slightly. Figure 5.1d shows that the melting temperature for Sn-9Zn-0.7Cu is 199.33^{0}C which is 2^{0}C higher than the eutectic solder alloy. Table 5.1 shows the melting and liquidus temperature for different solder alloys.

Table 5.1 Melting and Liquidus Temperature for different solder alloys

Material	Melting Temp ^{0}C	Liquidus Temp. ^{0}C	Heat Flow. W/g
Pure Sn	229 23	239.38	6.594
Sn-9Zn	197.59	201.77	1 765
Sn-9Zn-0.5Al	197.48	203.26	0.8431
Sn-9Zn-0.7Cu	199.33	201.11	2.293

5.2.2 Effect of Various Cooling Rates on Sn-9Zn Solder Alloy

Almost all soft solders are of binary or ternary alloys of Sn. Elemental Sn melts at 231^{0}C and is alloyed with other metals to create both lead-based and lead-free solders with the desirable mechanical properties. White, or β-Sn, has a body-centered tetragonal crystal structure and is stable at room temperature. The eutectic composition of the Sn-Zn binary system occurs at Sn-9Zn. The eutectic temperature is 198^{0}C. The microstructure consists of β-Sn and α-Zn rich phases in the form of thin platelets or needles. The impact of cooling rate changes the phases present in the solder microstructure. The shear strength is generally improved by a fast cooling rate. Slow cooling produces a near equilibrium, uniform lamellar eutectic structure that tends to increase the ductility The impact of work hardening resulting from higher strain rates tends to have a larger impact on the fast cooling samples [72]

The impact of cooling rate was observed on Sn-9Zn binary eutectic solder alloys. The cooling rates were varied from 5^{0}C, to 25^{0}C/minutes for this experiment. First the samples were heated up to 250^{0}C in a differential scanning calorimeter and then cooled with various rates to observe the effects. A summary of the cooling history is listed in the table 5.2. As the cooling rate slows down from 25 to 5, the under-cooling also decreases from 11.82^{0}C to 9.20^{0}C and as well as the energy absorbed decreases

from 7.221 W/g to 2.271 W/g. For 5^0C/minutes the onset point found at 191.81^{0}C, whereas the onset point for 25^0C/minutes was at 186.9^{0}C

Table 5.2 Effect on melting behavior for different cooling rates

Cooling Rate ^{0}C/min	Onset point, On cooling ^{0}C	Peak point on cooling ^{0}C	Peak point on heating ^{0}C	Under Cooling ^{0}C	Heat Flow on cooling W/m
5	191.81	195.20	204.75	9.20	2.271
10	190.17	194.00	205.65	11.65	3.802
25	186.90	192.32	204.14	11.82	7.221

The microstructure also changes due to the various cooling rates. It is well expected that the grain size will be thick for slow cooling rate and will be fine for faster cooling rate. In this experiment, although the cooling rates were only 5^0C apart, there is a significant change observed in the microstructure for different cooling rate in eutectic Sn-9Zn alloy. Figure 5.2 shows SEM images in SE mode for samples cooled at different rates. It is well known that slow cooling produces a near equilibrium structure which is full of thick eutectic lamella

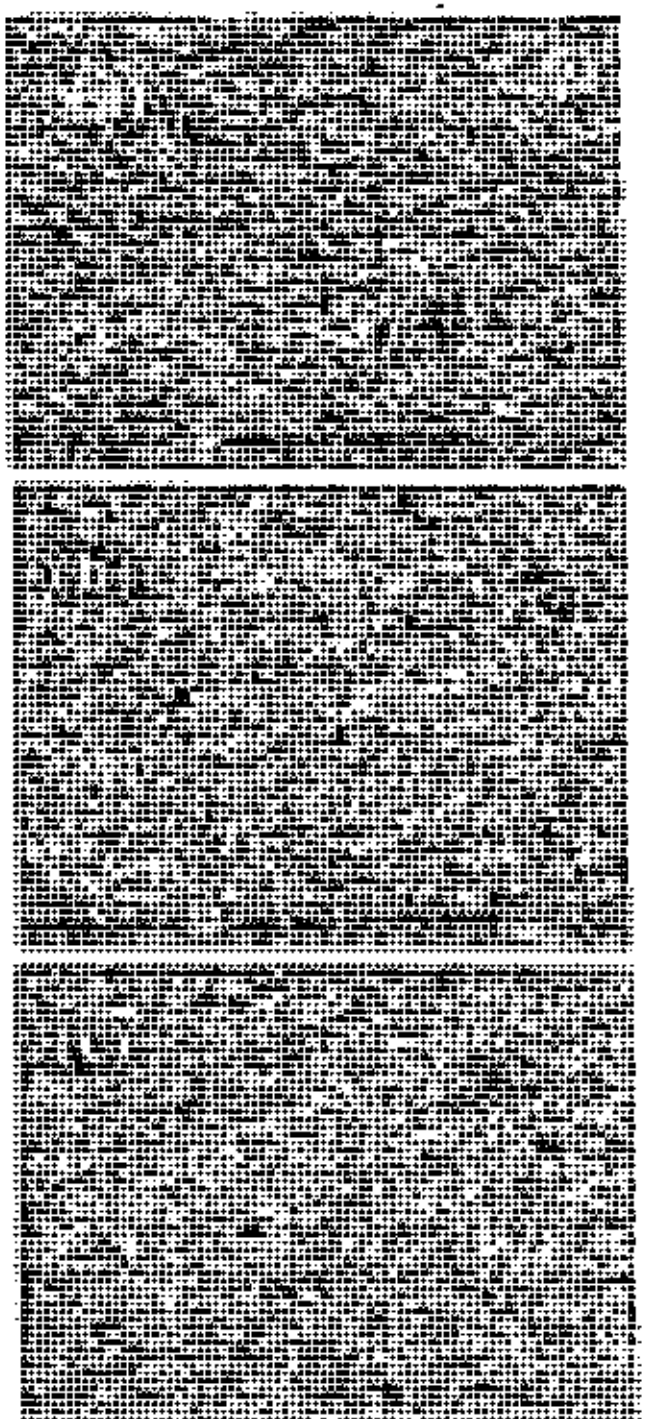

Figure 5.2 SEM microstructure of Sn-9Zn samples after various cooling rates (a) 5^0C/min, (b) 10^0C/min, and (c) 25^0C/min

5.3 MICRO HARDNESS

The measurement of hardness, especially microhardness, is a usual method to characterize the mechanical properties of solid-state surfaces. The hardness of the material is often equated with its resistance to abrasion or wear and its characteristic of practical interest since it determines the durability of a material during use and it also decides the suitability of the material for special applications. Microhardness tests are made to determine the hardness of individual grains, phase and structural component of alloys. In this case, the volume deformed through indenting should be smaller than the volume of the grain to be tested. For this reason, a light force is applied to the indenter. The microhardness of a solder alloy depends on the motion of dislocation growth and configuration of grains. The processes are more sensitive to the microstructure of the solder than its chemical composition. So the mechanical property such as the microhardness depends especially on the microstructure, processing temperature, the composition and so on [73]. In general, the hardness of the Sn-rich Pb-free solders strongly depends on the alloying elements; the more alloying elements there are, the higher the hardness is

The microhardness measurement in the present study was performed on the samples using a Vickers Shimadzu microhardness tester. Before indentation testing, necessary grinding and polishing were done to obtain a polished, smooth and flat parallel surface The applied load was 50g for 10s and 7-10 readings of different indentation were taken at room temperature to obtain the mean VHN value.

The results obtained of the microhardness at small load of the pure metal Sn and the Sn-9Zn, Sn-9Zn-0.5Al, Sn-9Zn-0.7Cu solder alloys are presented in Figure 5.3 It has been known [74] that the micro-indentation hardness of some materials (e.g. metals) is a constant above a critical size of impression but below this size a steady increase in hardness occurs as load is decreased. Buckle [75] has suggested that it is the presence of covalent regions in such materials that is responsible for the increase in hardness with decreasing load.

Several explanations have been put forward to account for the higher values of microhardness at lighter loads McClintock and Argon [76, 77] argue that at small loads, the impression size approaches to the slip band length at the equivalent strain, which increase the hardness value. Also, the strain gradients around the impression may require dislocation densities larger than those normally encountered in cold-worked metals at comparable levels of strain. Meyers and Chalwa [78] point out that the work hardening introduces in the surface by polishing may be important at lighter loads. Dieter [79] argues, on the other hand. that for lighter loads the impression is considerably affected by small amount of elastic recovery, which is normally negligible for higher loads.

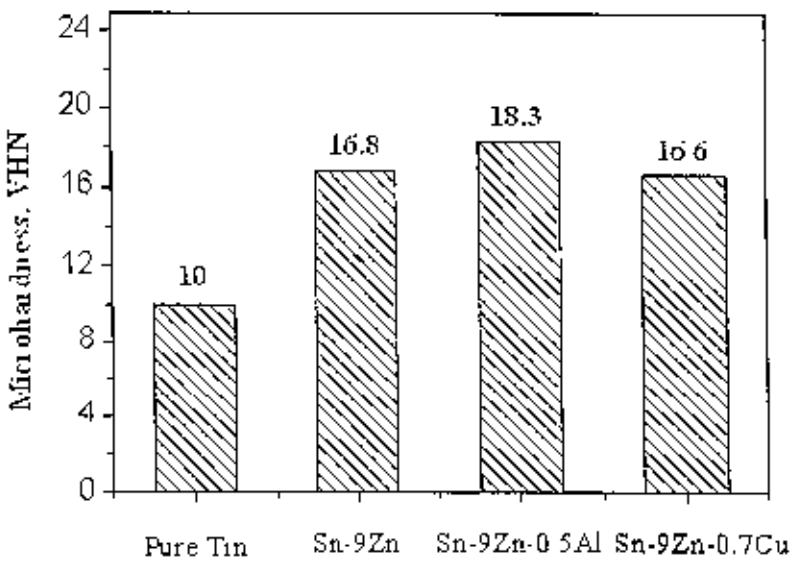

Figure 5.3 Microhardness values in terms of Vickers Hardness Number for different solder alloys

Braunovic [80] proposed that the mechanism for load dependence of indentation hardness is associated with the movement of dislocations introduced by the indenter. The generation of dislocations at a contact surface can be visualized a arising from a punching and blocking of dislocation may impede this movement by lattice defects

such as grain boundaries, vacancies, solute atoms, precipitates and similar imperfections in crystalline solids.

As shown in Figure 5.3, an increase in microhardness for Sn-9Zn eutectic solder than that for pure Sn was observed due to the presence of rod or needle-like Zn-rich phase in the β-Sn matrix. For the case of Sn-9Zn-0.5Al and Sn-9Zn-0.2Cu ternary solder alloys, the microhardness value rises also due to the presence of Al_6Zn_3Sn, Cu_6Sn_5 and Cu_5Zn_8 particulates in the β-Sn solder matrix. This could be accounted by the dispersion-strengthening effect. Again a slight decrease of VHN is observed for Sn-9Zn-0.7Cu which may be due to the lack of thick eutectic lamella, as some of the Zn react with Cu to form IMC that left the β-Sn matrix deprive of dark α-Zn phases.

As reported previously [78], the hardness value for the intermetallic particulates and Zn-rich zone is much higher than β-Sn matrix.

5.4 TENSILE STRENGTH

5.4.1 Tensile test and specimen

The ultimate tensile strength (UTS) is the maximum engineering stress, which a material can withstand in tension, on the engineering stress-strain curve [81]. The yield stress is the stress level at which plastic deformation begins. For solder alloys, the yield stress is commonly defined by the stress on the stress-strain curve at 0.2% strain offset. It is also called the 0.2% proof stress.

The tensile specimens were prepared by the mechanical machining of chill-cast ingots. They have a gauge length marked 25.00mm for each samples, the width and thickness for each samples are 6.00mm and 5.00mm respectively as shown in Figure 5.4. Tensile tests were carried out on an Instron testing machine (Instron 3369 Universal Testing Machine) at a rate of 1.00mm/min at 298K to obtain data on the stress-strain curves which contain information of elongation at fracture and the UTS.

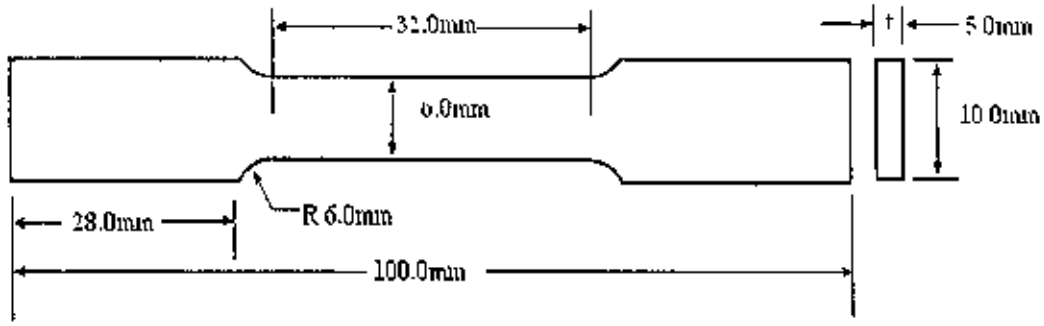

Figure 5 4 Schematic diagram of the tensile specimen.

5.4.2 Tensile property of the Sn-9Zn-X alloy

With the addition of Al and Cu in the Sn-9Zn alloy, it is expected that its mechanical properties will be improved due to the modification of the microstructure as mentioned in the previous chapter. According to dispersion strengthening theory if a second reinforcing phase is present in any structure, then the stress acting on the particle's surface can be expressed with the piling-up of linear dislocation, i. e. [79]

$$\tau = n\tau_0$$

Where τ is the stress at the particle surface, n is the piled-up dislocation number, and τ_0 is the yielding stress of the alloy. Meanwhile, the piled-up dislocation number is

$$n = \frac{\pi(1-\upsilon)L\tau_0}{Gb}$$

Where L is the average distance between the second phase particles, b is the Burgers Vector, υ is the Poisson's ratio, and G is the shear elastic modulus of the substrate.

Therefore, $\tau = \frac{\pi(1-\upsilon)L\tau_0^{\,2}}{Gb}$

and the yielding stress of the alloy becomes $\tau_0 = \sqrt{\frac{Gb\tau}{\pi(1-\upsilon)L}}$

If we assume that τ is the fracture stress of second particles and υ as a constant, the yield stress of the alloy increases when the average distance between the secondary particles decreases. Therefore, the fine-dispersion of secondary particles can enhance the strength of the alloys.

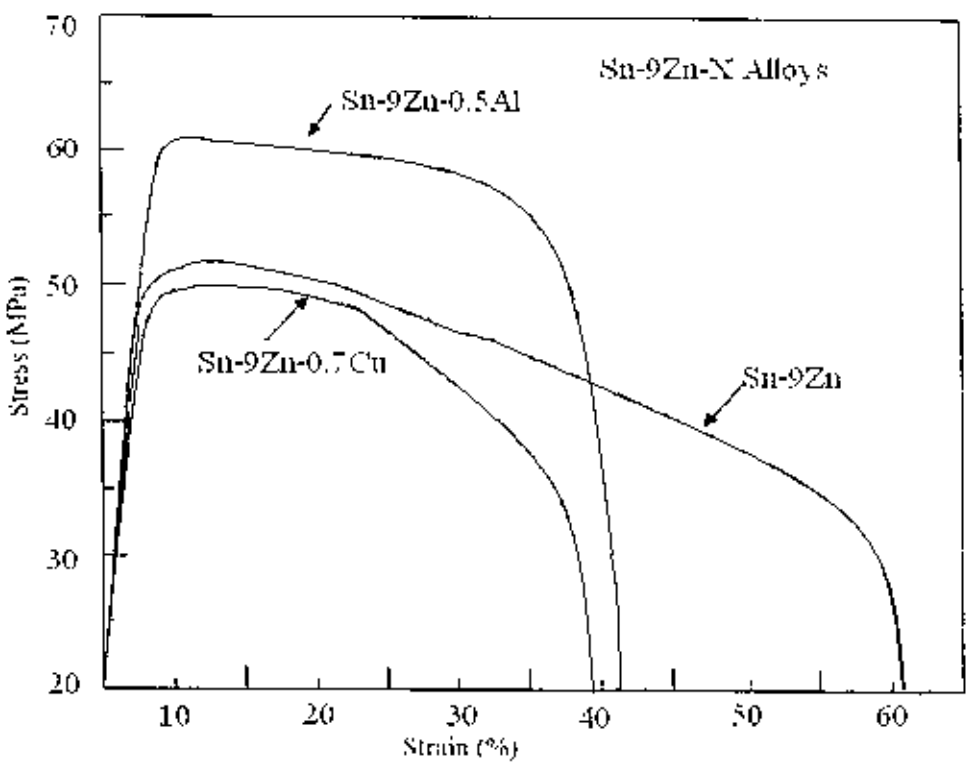

Figure 5.5 Tensile stress-strain curves of Sn-9Zn, Sn-9Zn-0.5Al, and Sn-9Zn-0.7Cu alloys.

Figure 5 5 shows the typical stress-strain curves of Sn-9Zn, Sn-9Zn-0 5Al, and Sn-9Zn-0 7Cu alloys. A significant improvement of the tensile strength is observed for Al addition, whereas a decrease in the strength occurs for Cu addition in Sn-9Zn binary eutectic alloy. But the ductility decreases with the addition of both Al and Cu.

Figure 5.6 shows the tensile properties for Sn-9Zn, Sn-9Zn-0.5Al, and Sn-9Zn-0.7Cu alloys. An increase in 21% of the proof strength is observed for Al addition in Sn-9Zn alloy, as well as a 32% drop in elongation is observed for the same. For Cu addition both the proof strength and elongation decreases 6.6% and 38% respectively.

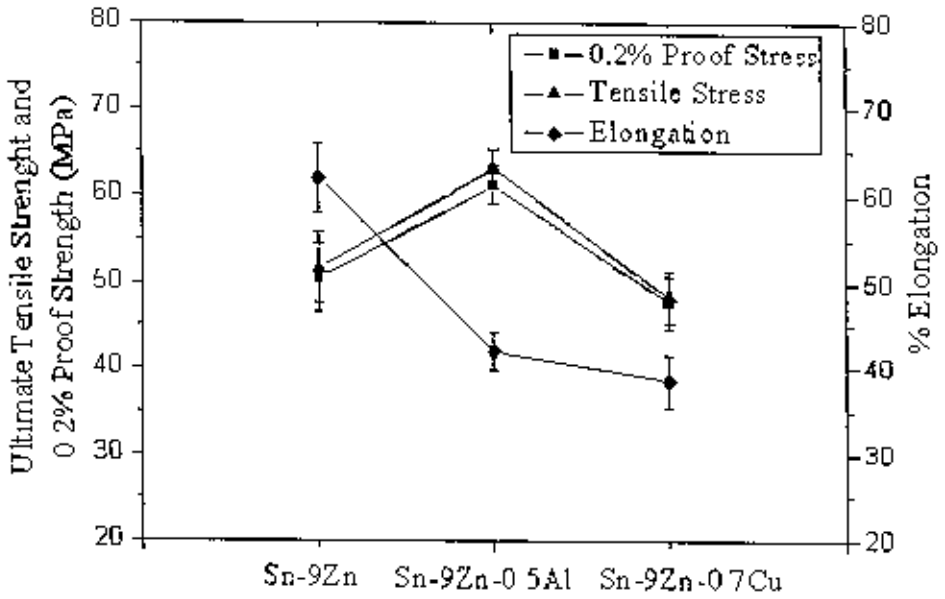

Figure 5.6: Tensile properties of Sn-9Zn, Sn-9Zn-0.5Al, and Sn-9Zn-0.7Cu.

As per dispersion strengthening theory, the strength must increase with the addition of a second phase particle in the matrix. And for the case of Al addition in Sn-9Zn the theory proved right, while for Cu addition the theory contradicts with the results. These contradiction can be explained from the microstructure and as well as the tensile fracture surface of the alloys very clearly. As discussed in the previous chapter, some small precipitates observed in the microstructure of Sn-9Zn-0.5Al, which are uniformly distributed in the solder matrix and also the palate-like Zn-rich phase becomes finer. While some flower and rod shaped large intermetallic compounds were observed in Sn-9Zn-0.7Cu alloy and also the dark Zn-rich phase

decreases from the matrix. According to Dieter [79], the second phase element increases the tensile strength up to a certain extent and beyond that the precipitate starts to grow non-coherently which results in the decrease of the overall strength. And for the case of Sn-9Zn-0.7Cu the IMCs growth is beyond that limit which results in a decrease in the tensile strength.

Figure 5.7 shows the fractography of the alloys after tensile tests. All alloys displayed a typical ductile fracture mode. The dimpled pattern is present in all the fracture surfaces. The dimple size of the alloys varies for different elemental content. The dimples size for Sn-9Zn-0.5Al is much finer than that of other two alloys Especially, in the case of Sn-9Zn-0.5Al and Sn-9Zn-0.7Cu alloys, some Al–Zn-Sn and Cu–Zn compounds were observed in the fracture surfaces The fracture surface of the Sn-9Zn-0.5Al alloy shows many fine dimple structures (Figure 5.7 b) On the other hand, the fracture surfaces of the Sn-9Zn-0.7Cu alloy exhibit cleavage patterns, as shown in Figure 5.7 c. Thus, Sn–9Zn–0.7Cu alloy undergoes a complex fracture pattern. From the results of tensile tests on Sn–9Zn–0.5Al alloy, the formation of Al–Zn-Sn compounds promote tensile strength and deteriorate elongation slightly, while the tensile tests for Sn–9Zn–0.7Cu alloy reveal that the Cu–Zn compounds deteriorates both tensile strength and elongation.

Figure 5.7: SEM fractrograph in SE modefor (a) Sn-9Zn, (b) Sn-9Zn-0.5Al and (c) Sn-9Zn-0.7Cu

5.5 CONCLUSION

With the addition of 0.5% Al addition the melting temperature does not change significantly from that of the Sn-9Zn alloy, as the ternary eutectic Sn-9Zn-0.45Al alloy exhibit its melting point at 197^{0}C. But, when 0.7% Cu is added into Sn-9Zn alloy, the melting temperature jumps 2^{0}C higher than the original melting temperature of Sn-9Zn binary eutectic solder. Thus, adding a small amount of Al; the soldering temperature can be kept as original one. Cooling rates have significant effect on the microstructure and properties of any alloy. For the case of Sn-9Zn binary eutectic alloy; fast cooling results finer and more uniform microstructure with dispersed needle-like Zn-rich phase in the β-Sn matrix, whereas slow cooling results in a coarse dendrite structure with rod-like Zn-rich precipitates. Due to the refinement of microstructure when adding Al and Cu into the Sn-9Zn solder alloy, it is reasonable to see an improvement in the microhardness for the ternary alloys. The increase in microhardness is believed for the IMCs formed by Zn with Al and Cu, which posses much higher hardness than the eutectic lamella. When the Al is added the tensile strength improved on the other hand elongation decreased. The both phenomenon can be clearly explain by the dispersion strengthening theory; i.e. the second phase formed by aluminum generates obstacle for the dislocation at the grain boundary (the maximum region of mismatch), dislocation pile up results in a increase in tensile strength, the term also called precipitation strengthening. On the other hand due to movement restriction of dislocation densities, the slip planes can't find their suitable direction to move freely results lack in ductility; i.e. elongation decreases. For copper addition in Sn-9Zn eutectic solder alloy tensile properties deteriorates. Both tensile strength and elongation decreases significantly. The tensile strength falls due to addition of copper is believed for the non-coherent precipitation of Cu_5Zn_8 and Cu_6Sn_5 intermetallic compound. This big IMCs show non coherency with the β-Sn matrix, which in turn decrease the tensile strength. Elongation also falls due to the same reason of suitable slip plane movement restriction. Thus, both toughness and elongation decreases with the addition of a third element in Sn-9Zn binary eutectic solder alloy.

CHAPTER 6

COMPOSITE SOLDER

6.1 INTRODUCTION

Composite approaches have been developed in lead-free solder research in an effort to improve the service temperature capabilities and thermal stability of the solder joints. Several challenges are faced in the development of lead-free solders since they are not just drop-in substitutes for traditionally used leaded solders. These challenges may be related to the solder melt temperature, processing temperature, wettability, mechanical and thermo-mechanical fatigue (TMF) behaviors, etc. Knowledge base on leaded solders gained by experience over a long period time is not directly applicable to lead-free solders. Thus, most of the lead-free solder developments for electronic applications are aimed at arriving at suitable alloy compositions.

6.2 EXPERIMENTAL PROCEDURE

In the present study, the compositions of the composite solder alloys were prepared were Sn-9Zn with 0 wt. % to 4 wt. % Ag micro particles. A commercially-available eutectic Sn-Zn solder paste was mixed with the Ag micro-particles. The average size of the Ag particles were about 8-10μm. The mixing technique was adopted to add the Ag micro particles in the Sn-Zn eutectic solder paste. The composite mixture was then blended around 30 minutes by hand to achieve a uniform distribution of the reinforcements. Then the mixed paste was screen printed on a polished alumina plate. The alumina plate with the printed solder paste on it was then reflowed at a temperature of 240^0C in a convection reflow oven (BTU VIP-70N) to prepare the composite solder balls.

The thermal analysis of the alloys was carried out using a differential scanning calorimeter (2190-MDSC) in the temperature range from room temperature to 230^0C

in a nitrogen gas flow of 50 ml/minute The heating rate was 25Kminute^{-1} up to 150^{0}C which was then equilibrated there for one minute, finally 10Kminute^{-1} up to 230^{0}C.

A solder mask-defined copper bond pad on a BGA package was used as a base for electro-deposition of Ni and Au. The solder mask-opening diameter was 0.6 mm with 7-μm thick Ni on the ball pad. The average thickness of the Au layer was 0.5 μm. The lead-free composite solder balls with an average diameter of 0.70 mm were placed on the pre-fluxed Au/Ni/Cu bond pads of the substrates and reflowed at a temperature of 250^{0}C for 1 minute to examine the interfacial reactions between the solder and the thin-film under-bump metallurgy (UBM). The flux used in this study was a commercial rosin activated flux (A88, Alpha Metals Ltd. HK).

Shear tests were performed for the as-reflowed samples using a Dage (Dage Holdings Ltd., Aylesbury, UK) Series 4000 Bond Tester. The shear tool height and the test speed of the shear test in this study were about 20 μm and 550 μm/s, respectively. The test load for shear was 5000 g for every test. About 40 randomly chosen solder balls were sheared to obtain the average and the extent of deviation for each composition.

Another set of composite solder balls were placed on a highly polished pure copper sheet and reflowed at 250^{0}C to find the wetting behavior. Finally, the spread of different solder balls was measured under an optical microscope with digital a camera (LEICA-MZFLIII) to find the effect of the Ag particles on the spreading behavior.

The fracture surfaces after the ball shear tests were investigated thoroughly using a Philips scanning electron microscope (Eindhoven, The Netherlands) XL 40 FEG (SEM) in the secondary and backscattered electron mode as well as by energy dispersive X-ray spectroscopy (EDX). To investigate the microstructures and intermetallic layers at the interface, the as-reflowed samples were mounted in resin, cured at room temperature, mechanically ground, and then polished with 0.5 μm

Al_2O_3 powder in order to obtain the cross sections of the solder/UBM interfaces. The chemical and microstructural analyses of the gold-coated cross-sectioned samples were obtained using the SEM equipped with an EDX spectrometer. The accuracy of the compositional measurement was about ±5%. To determine the formula composition of the intermetallic compounds (IMCs), the chemical analyses of the EDX spectra were corrected by standard ZAF software. The backscattered electron imaging mode of the SEM was used for the interfacial study

6.3 RESULTS AND DISCUSSION

6.3.1 DSC analysis

DSC analyses were carried out in order to investigate the fundamental thermal reactions on heating of the composite solder alloys and also to find the sustainable range for these composite solders. Fig 6.1 shows typical DSC curves obtained for Sn–9Zn based Ag particulate composites on heating

On heating, the prominent endothermic peak for all composite solders appeared at around 201^0C, which corresponds to the eutectic temperature of the Sn–Zn binary system. An addition of Ag particles shifted the endothermic peak from 199^0C to slight higher temperature. It has already been proven that the liquidus line of the Sn–Zn eutectic alloy rises with an increase in the Ag content [82]. It is noteworthy that the height of the first peak decreases with an increase in the Ag content. It is also interesting that a shoulder was observed at around 210^0C for 3% and 4% Ag containing solders.

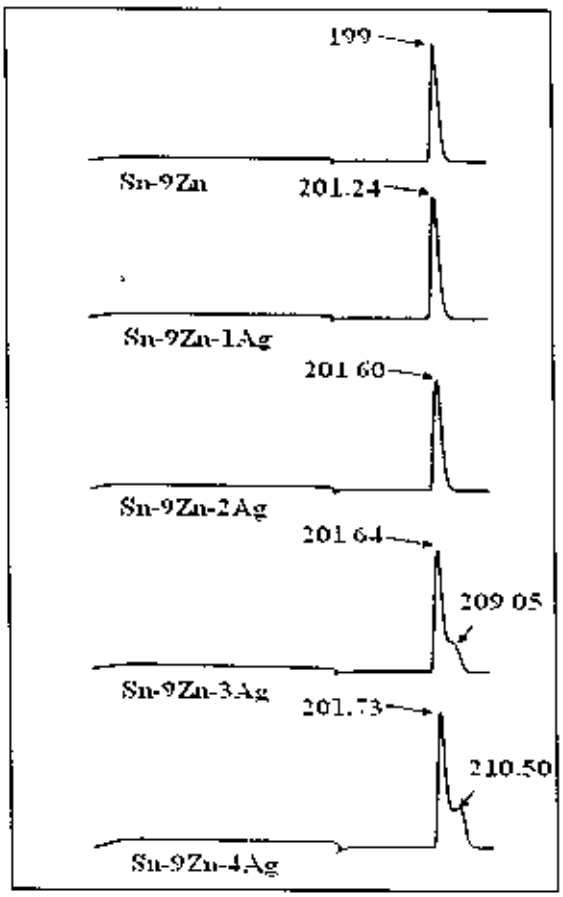

Figure 6.1 DSC curves of Sn-Zn-Ag micro-composite solder alloys on heating.

6.3.2 Shear Strength

The interfacial reactions between the Pb-free solders and the electrolytically deposited Au/Ni/Cu bond pads were conducted by holding at 250^{0}C for 1 minute. The mechanical strength of the interface was measured for each different solder composition. The change of the average shear loads and their standard deviations are shown in Fig. 6.2.

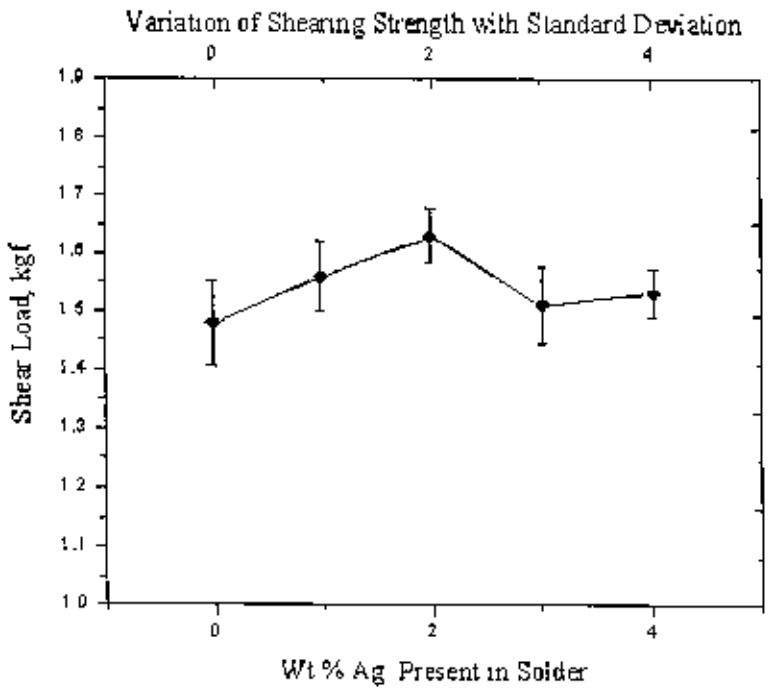

Figure 6.2 Variation of average shearing forces with standard deviation of solder joints for different proportion of Ag micro-particles in Sn-Zn composite solder.

It may be noted that the average shear strength of joints increased with the Ag micro-particle content up to a certain limit. Beyond this limit, the addition of Ag particles actually decreased the joint strength. Overall the composite solders showed a higher shear strength than the eutectic Sn-Zn solder. The average shear loads of the solder joints were around 1.53 kgf, 1.51 kgf, 1.63 kgf, 1.56 kgf and 1.48 kgf for 4, 3, 2, 1 and 0 wt. % Ag content in the Sn-Zn eutectic solder, respectively. For the 2 wt. % Ag particle content in the Sn-Zn eutectic solder, the shear load was higher than the rest of the compositions in the as-bonded condition on the electrolytic Au/Ni surface finish. With more than 2% addition of Ag, the joint strength decreased again.

The fractured surfaces of the pads and sheared balls were immediately studied by SEM. The results reported here (from fracture surface and cross-sectional studies) are based on the highest number of similar occurrences from each readout point of shear

strength data. In most cases ductile fracture occurred within the solder for the reflowed samples. For 1% and 2 % Ag containing composite solder alloys, the fracture occurred at a location near but lower than the shearing height (20 μm), leaving a thick layer of solder on the pad. This indicates that the solder/pad bond is stronger than the bulk solder. Fig. 6.3 shows a fracture surface of the interface formed between a 2% Ag containing composite Sn-Zn solder alloy and a electrolytic Au/Ni/Cu bond pad after reflow at 250°C for 1 minute.

The EDX analysis from these surfaces proved that fracture occurred through the solder alloys. From the EDX analysis (Fig. 6.3d) it is also confirmed that the dark spots shown in Fig 6.3c are actually $AgZn_3$ IMCs and the bright irregular surfaces are mostly a Sn-rich phase. In the case of Sn-9Zn eutectic solder the fracture morphology was also similar, but from the EDX analysis of the fracture surface it was clear that here the Zn content was higher compared to the other composite solders.

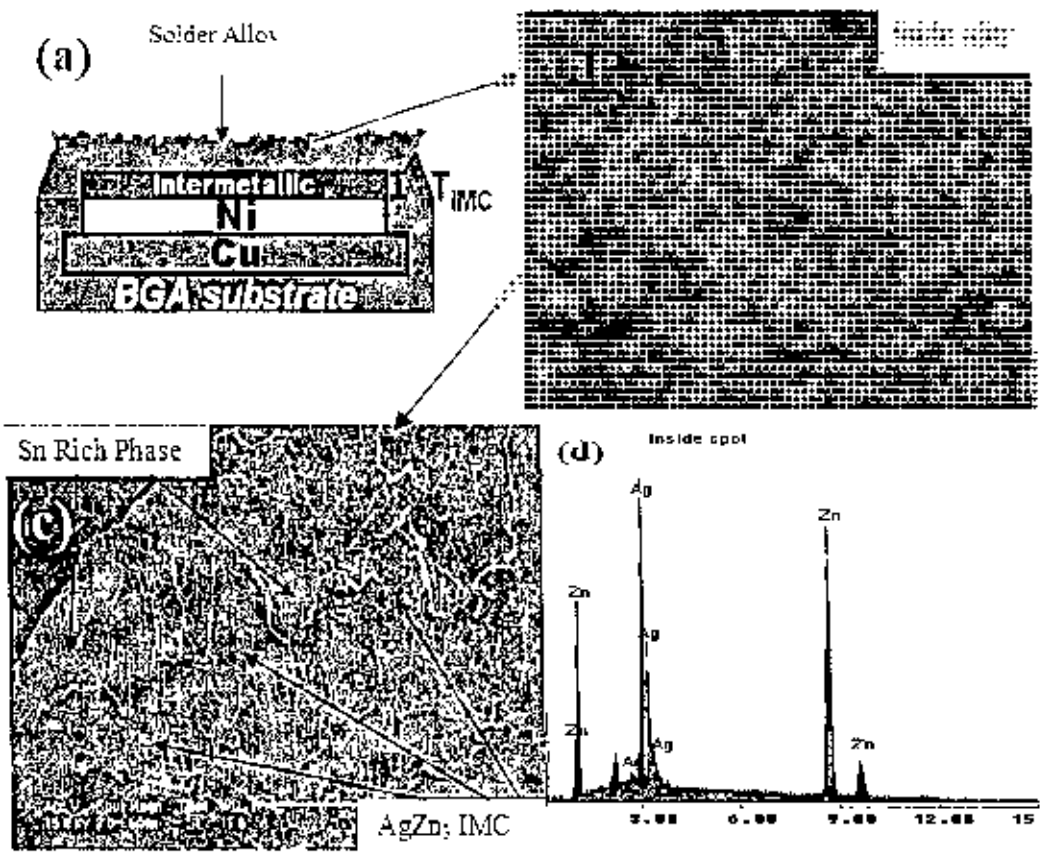

Figure 6.3 (a) Schematic drawing of the shearing fracture mode of a BGA solder joint. (b) Fracture surface of the Sn-Zn-2Ag solder joint after 1 minute of reflow at 250^{0}C. (c) Enlarged view of the fracture surface showing $AgZn_3$IMC. (d) The EDX of the black spots inside the matrix.

For composite solders containing more than 2% Ag, the fractures were mainly ductile with few occurrences of a mixed mode of both ductile and brittle fracture as shown in Fig. 6.4.

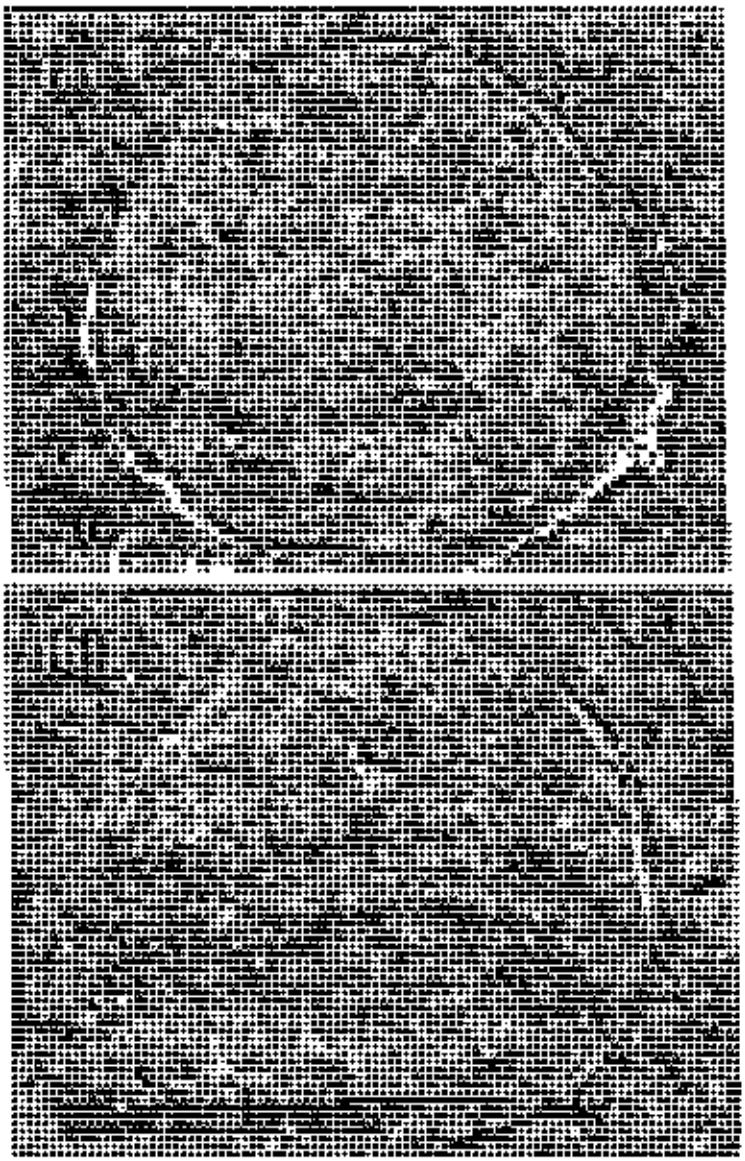

Figure 6.4 Fracture surface for (a) Sn-Zn-3Ag; (b) Sn-Zn-4Ag; composite solder joints after 1 minute of reflow at 250^{0}C.

6.3.3 Bulk Solder Matrix

The distribution of Ag rich-particles in the Sn-Zn matrix was found to be reasonably homogeneous in the composite solders prepared from the Sn-Zn paste and the Ag particles (Fig. 6.5). The Ag micro particles in the bulk solder reacts with the Zn

surrounding to them and form dark ϵ-$AgZn_3$ "flower" like IMC compound particles on the surface of the Ag micro particle as shown in Fig. 6.5.

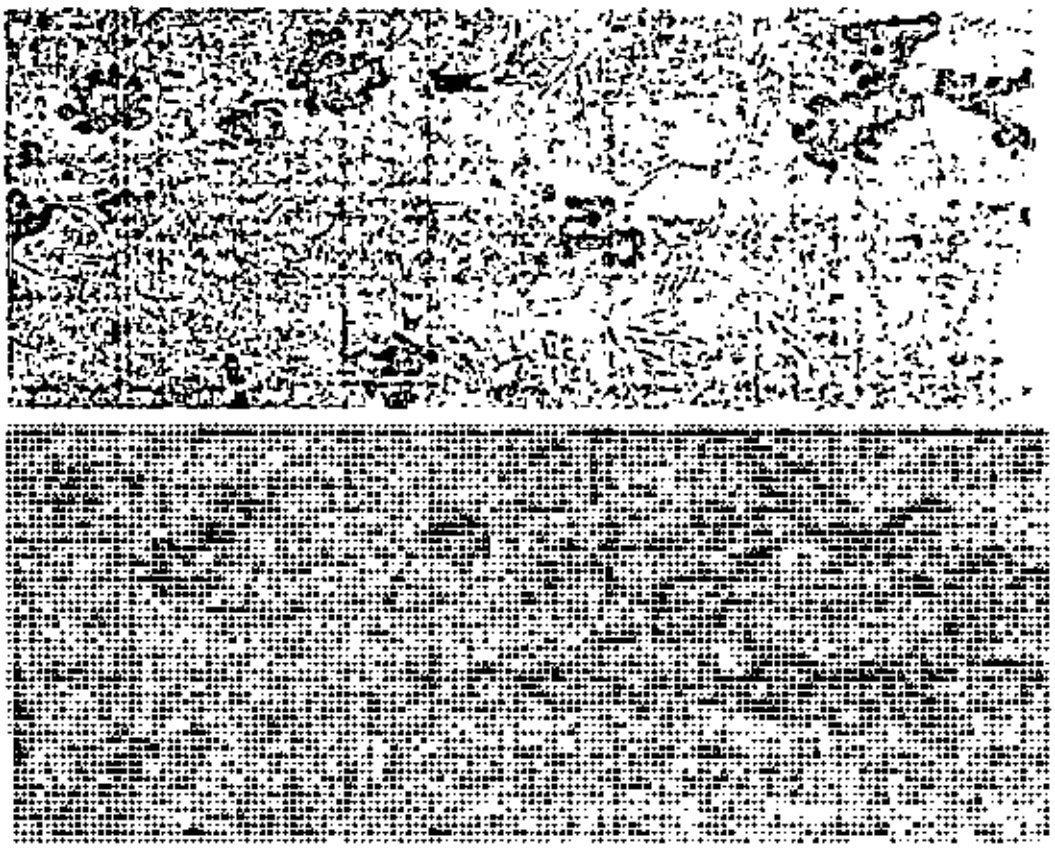

Figure 6.5 Matrices of composite solder alloys with uniformly distributed "flower" like $AgZn_3$ IMCs (a) Sn-9Zn-4Ag, (b) Sn-9Zn-3Ag, (c) Sn-9Zn-2Ag, (d) Enlarged view of a "flower" like IMC particle inside the bulk solder matrx composition Sn-9Zn-3Ag.

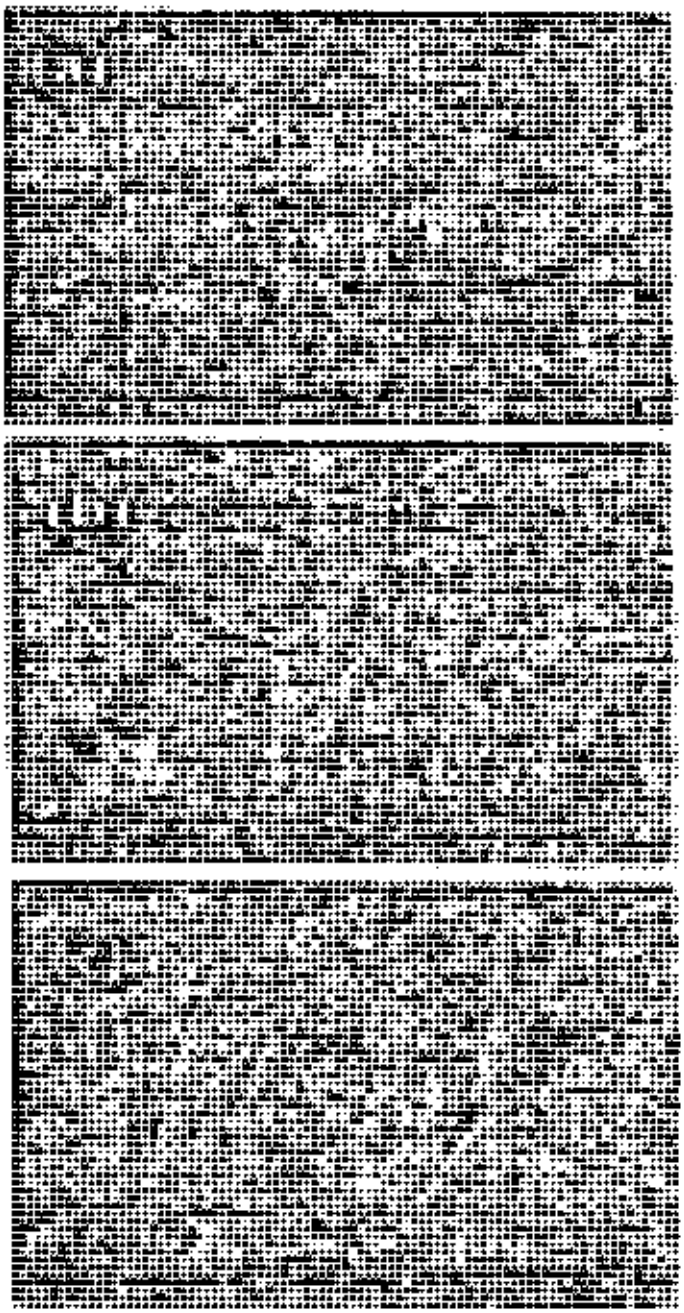

Figure 6.6 Matrices of composite solder alloys at higher magnification showing depletion of α-Zn phases (which is the phase in darker gray contrast) (a) Sn-9Zn-4Ag, (b) Sn-9Zn-2Ag, (c) Sn-9Zn.

The core of the compound particle remains as pure Ag (lighter gray contrast-Fig 6.5d) As a result; the bulk solder matrix becomes depleted in Zn-rich phase with an increasing in the Ag micro particle content in the Sn-Zn eutectic solder as shown in the Fig. 6.6.

The addition of larger amount of Ag into the solders resulted in the formation of larger amount of $AgZn_3$ compound. This reaction reduced the Zn content of the eutectic Sn–Zn composition which formed a hypoeutectic β-Sn structure [83]. Thus, the endothermic peak of the solders investigated resulted from two transformations. One was the melting of the eutectic Sn–Zn and the other was the melting of the hypoeutectic β -Sn. In the DSC curves in Fig. 6.1, the appearance of the shoulder for 3 and 4% Ag containing solders was the result of the formation of this hypoeutectic β-Sn.

6.3.4 Interface between Composite Solder and Au/Ni/Cu Bond Pads

Detailed cross-sectional studies were carried out to investigate the relationship between the shear strength and the interfacial morphologies of the solders with the Au/electrolytic Ni/Cu pads.

All interfaces, to a greater or lesser extent, reveal similar features-solidified solder, reaction zone, original electrolytic Ni layer, and Cu pad. Most interestingly, a layer-type spalling at the interface was clearly observed in the Sn-Zn solder system from the initial reflow (Fig. 6.7a). EDX analysis of this spalled IMC layer revealed that the IMC was composed of Au and Zn and the Au percentage of this layer was about 25 at. %. This observation implies that the spalled IMC layer is made up of the $AuZn_3$ compound. A very thin layer of IMC was also noticed at the interface of the Sn-Zn solder system The active nature of the Zn confirmed an instant reaction zone at the interface to maintain the bonding between the solder and the substrate.

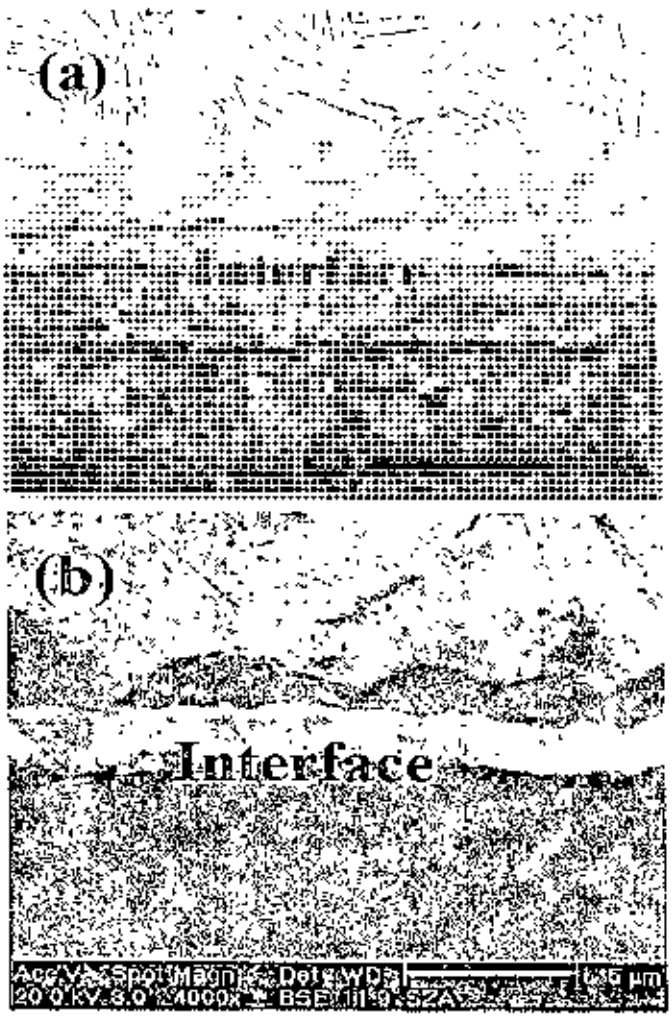

Figure 6.7 (a) Spalling of the initial IMC for the Sn-9Zn eutectic solder alloy sample.

(b) A two-layered IMC structure at the interface for the Sn-9Zn-1Ag composite solder alloy sample.

With the addition of 1%Ag, no severe spalling of the initial IMC from the pad surface was noticed at the interface of the Sn-Zn composite solder/Ni system. On the other hand, there were places along the interface with no spalling. But some spalling of the IMCs was confirmed at some other places along the interface (Fig. 6.7b). A two-layered IMC structure was observed on the electrolytic Ni layer. The white thick

layer was composed of Au, Zn and Ni. The upper grey layer was composed of Ag and Zn with a small amount of Au

With 2-4% Ag, no spalling of the initial IMCs was observed at the interface. On the otherhand, three distinct IMC layers were formed at the BGA bond pad and composite solder interface. These three different IMC layers were also different in chemical composition. Another important thing is that the Au does not dissolve into the Sn-Zn based solders. Instead, Au formed an IMC layer at the interface. The EDX analysis of the three IMC layers revealed that in the lower two IMC layers Au reacted with Sn & Zn to form different compounds which form different compounds

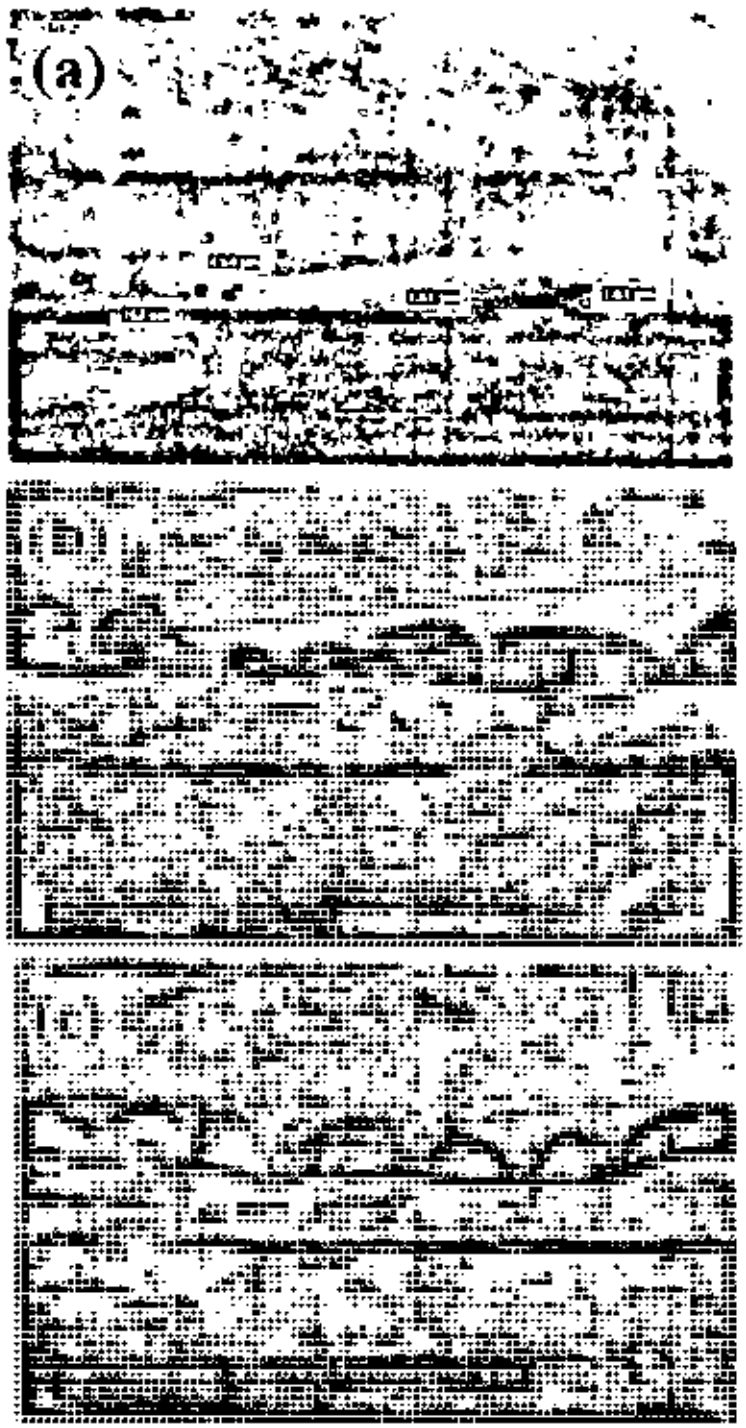

Figure 6.8 Three distinct IMC layers at the interface for composite solder alloys with thickness as marked; (a) Sn-9Zn-4Ag, (b) Sn-9Zn-3Ag, (c) Sn-9Zn-2Ag.

Fig. 6.8 shows the three distinct IMC layers produced by the Au/Ni/Cu bond pad with 2-4% Ag additions Sn-Zn-solder alloys From this figure it is clear that the top most layer towards the bulk solder is comparatively darker (in contrast) than the other two IMC layers. The EDX results show that this layer is mainly composed of Ag and Zn

From the EDX analysis the percentage of Ag found here is also about 25 at.% This observation implies that this IMC layer is the ϵ-Ag_3Zn_5 compound The morphology of these layers is mainly scallop type. As the Ag content increases in the Sn-Zn eutectic solder, the thickness of this scallop type IMC layer also increases. The topmost Ag-Zn IMC layer thickness for 1 wt.% Ag was 2.65μm, which gradually increases to 4.54μm for a 4 wt.% Ag micro particle addition.

The intermediate white IMC layers in Fig. 6 8 are made of Au and Zn. From the EDX analysis the percentage of Au found here is about 25 at.%. The thickness of these white layers remains almost the same for all the compositions at around 1 5 μm. Finally the third light dark IMC layer in Fig. 6 8 which is adjacent to the Au/Ni/Cu bond pad contains Zn, Au. Sn and a small amount of Ni. From the EDX analysis the average composition of the interfacial IMC layer near the substrate side was determined to be 55–63Zn, 14–23Au, 17-19Sn, and 3–9Ni (at.%).

It was confirmed that the Au-Zn IMC layer began to spall-off from the interface of the Sn-Zn eutectic solder and Au/electrolytic Ni/Cu system after the initial reflow [84]. During soldering, Zn atoms start immediately to react with Au atoms at the interface. The high surface tension of the Au-Zn compounds with the electrolytic Ni layer in the Sn-Zn solder may cause the Au-Zn layer to spall off from the interface in the molten state. The Ag particles in this experiment reacted with the molten solder (more precisely with the Zn therein) twice (firstly during ball preparation and secondly during the reflow soldering with the Au/ Ni pad) During these reactions, a Ag-Zn IMC formed on the outermost surface of the Ag particles which tends to dissolve away from the surface of the Ag particles. These dissolved Ag-Zn IMCs ultimately redeposited over the Au-Zn compound particles to prevent the whole IMC

layer lifting-off during reflow. With a 1% Ag addition, the formation and the redeposition of the Ag-Zn IMCs were insufficient to fully prevent the Au-Zn IMC layer spalling.

6.3.5 Spreading of Composite solder

The wetting/spreading behavior is also a very important issue for a solder. Thus, a comparative study spreading was carried out for the different solders. From Fig. 6.9 it is clear that the spreading of Sn-Zn eutectic solder decreases slightly with an increase the addition of Ag micro particles.

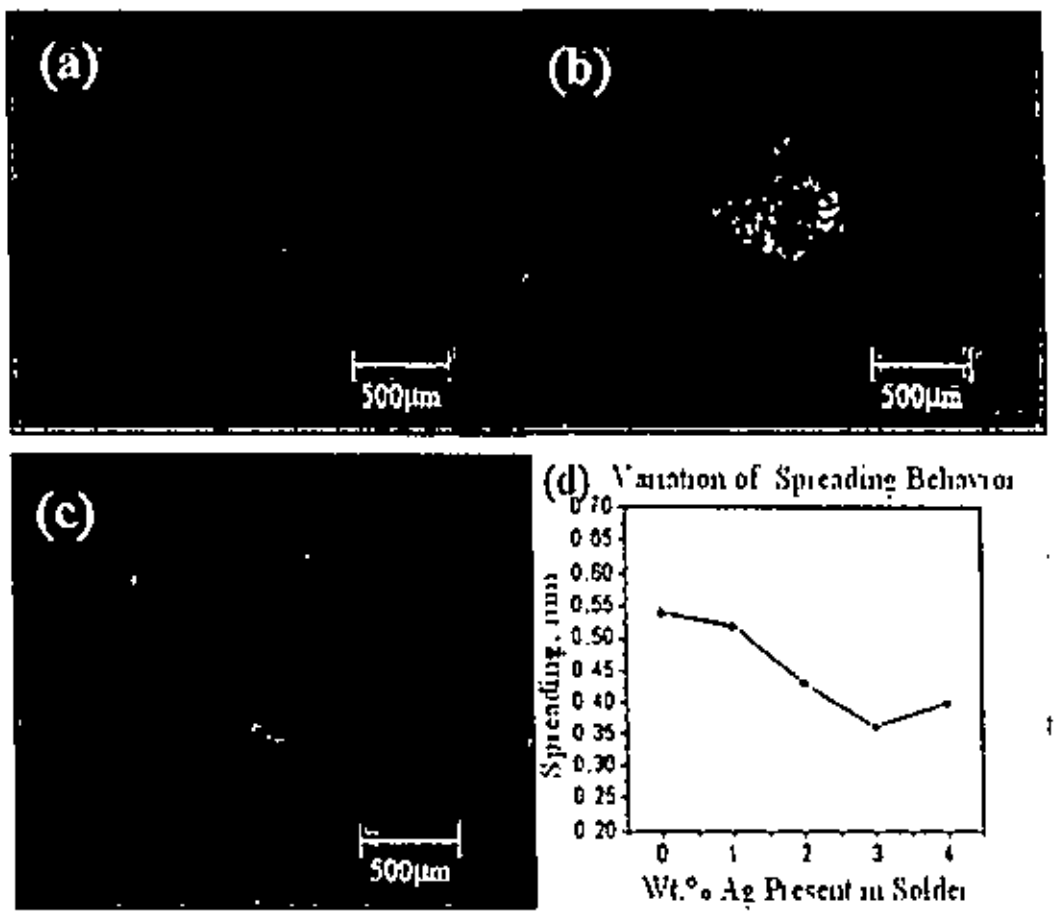

Figure 6.9 The solder balls after reflow at 250°C for 1 minute on Cu-sheets: (a) Sn-9Zn, (b) Sn-9Zn-2Ag, (c) Sn-9Zn-4Ag, and (d) Variation of their spreading behavior with an increase in the Ag content in the solder.

6.4 CONCLUSIONS

The addition of Ag particles in the Sn-Zn solder gave two major consequences. With the increase in Ag content, the uniformly distributed $AgZn_3$ coated Ag particles act as a reinforcing agent in the Sn-Zn matrix. The dissolved Ag-Zn IMC particles may also play some part in the composite structure. As a result the addition of Ag particles in the Sn-Zn alloy increased the shear strength of solder joints. On the other hand, with grater Zn consumption in the formation of Ag-Zn compounds, the bulk solder matrix became depleted in the eutectic α-Zn rich phase and resulting in more Sn-rich phase in the bulk solder. Again the initial spalling of the interface $AuZn_3$ IMC layers can be stopped by addition of Ag particles into the Sn-Zn eutectic solder which forms $AgZn_3$ IMC on the surface of the Ag micro particles in the bulk solder matrix which surfaces in turns redeposited on the former $AuZn_3$ layer. Thus the addition of Ag particles beyond a certain limit in the Sn-Zn systere actually decreased the strength of the solder joint. The Ag micro particles have almost no effect on the melting temperature of the Sn-Zn eutectic solder. From the above considerations, the Sn-Zn eutectic alloy with a additions of 2% Ag particles can be recommended as a possible replacement of the conventional Sn-Pb alloy for soldering in microelectronic applications.

CHAPTER 7

CONCLUSIONS AND SUGGESTIONS FOR FURTHER STUDY

7.1 CONCLUSIONS

The aim of this study was to improve the properties of Sn-9Zn eutectic solder which can be used as a replacement to conventional Sn-Pb solder. For this purpose small amount of Al and Cu were added to the Sn-Zn eutectic solder. The newly developed ternary solders were investigated for microstructural, mechanical, thermal and interfacial study for long-term soldering application. It was found that the newly developed Pb-free ternary solders had better performances than the eutectic binary Sn-9Zn solder.

The mechanical properties of solders were found to be highly dependent on their microstructure. It was found that the microstructure of the Pb-free solders studied in this research became refined by the addition of a third element through the size reduction of α-Zn phases and IMC particles. With the addition of the Al and Cu, the microstructures of eutectic Sn-9Zn Pb-free solders become more uniform than its original microstructure. The Al_6Zn_3Sn and Cu_5Zn_8 IMC were formed in the eutectic colonies when Al and Cu were alloyed with Sn-9Zn alloy, respectively. The reason for obtaining the uniform microstructure by the addition of a third element is that they promote a high nucleation density of the second phase in the eutectic colony during solidification. As a result, the refined microstructure exhibited better mechanical properties, such as higher ultimate tensile strength and microhardness. The improvement in tensile strength has to be traded off with the decrease in elongation.

To understand the melting behavior of the newly developed ternary Pb-free solder alloys, DSC analysis were carried out. It was found that with the addition of a trace amount of Al the melting temperature does not change significantly for Sn-9Zn alloy.

But, when a trace amount of Cu was added to the Sn-9Zn alloy the melting temperature increases about 2^0C compared to the original melting temperature of Sn-9Zn binary eutectic solder. Thus, adding a small amount of Al; the soldering temperatures can be maintained as its original one. We know that the cooling rates have significant effect on the microstructure and properties of any alloy, thus Sn-9Zn eutectic alloy was cooled at various rates with a differential scanning calorimeter and their microstructures were observed. It was found that fast cooling results in finer and more uniform microstructure with dispersed needle-like Zn-rich phase in the β-Sn matrix, whereas slow cooling results in a coarser dendrite structure with rod-like Zn-rich precipitates.

Now-a-days the composite approach is much popular in Pb-free solder development. Thus to understand the microstructural and mechanical properties, as well as the thermal behavior of the composite solder based on Sn-9Zn binary eutectic alloy, up to 4 wt % Ag micro particles were mixed with it. The addition of Ag particles in the Sn-Zn solder has two major advantages. With the increase in Ag content, the uniformly distributed $AgZn_3$ coated Ag particles act as a reinforcing agent in the Sn-Zn matrix. The dissolved Ag-Zn IMC particles may also play some part in the composite structure. As a result of the addition of Ag particles to the Sn-9Zn alloy the shear strength of solder joints is increased On the other hand, with greater Zn consumption in the formation of Ag-Zn compounds, the bulk solder matrix became depleted in the eutectic α-Zn rich phase and resulting in more Sn-rich phase in the bulk solder.

Interfacial study is the most important task in the soldering application. thus the interfacial reactions of Sn-Zn micro-composite eutectic solders with Au/Ni/Cu ball grid array (BGA) pad metallizations were systematically investigated. Results show that three distinct intermetallic compound (IMC) layers were formed at the interface of the Au/electrolytic Ni/Cu bond pads with the Sn-Zn composite solder alloys. The more Ag particles that were added to the Sn-Zn solder, the more Ag-Zn compound formed to thicken the uppermost IMC layer. The dissolved Ag-Zn IMCs formed in

the bulk solder redeposited over the initially formed interfacial Au-Zn IMC layer, which prevented the whole IMC layer from lifting-off the pad surface. The addition of Ag particles beyond a certain limit in the Sn-Zn system actually decreased the strength of the solder joint due to the depletion in the eutectic α-Zn phase and the Ag micro particles have almost no effect on the melting temperature of the Sn-Zn eutectic solder. Thus, the Sn-Zn eutectic alloy with an addition of 2% Ag particles can be recommended as a possible replacement to the conventional Sn-Pb alloy for soldering in microelectronic applications.

The above work shows that the Pb-free Sn-9Zn eutectic solder with a third element could be suitable for practical applications. However, there still exists some minor concern or limitations in using these ternary Pb-free solders in practical applications. First, the melting point of the Pb-free solders does not reduce with doping trace amount of Al and Cu. Soldering at high temperature may break down unprotected electronic components. Cost is another possible concern against the use of Ag-doped micro composite solders. Although the amount of Ag micro particles doped into Pb-free Sn-9Zn eutectic solder is very small, this would still increase the materials and production costs. It is because of the fact that additional processes are involved

Since both the Al and Cu both react with oxygen easily to forming oxides, it is difficult to use them in a solder bath for wave soldering and screen-printing in flip chip packaging. If the above-mentioned problems are improved or solved, it would be easier to adopt their use in industry.

7.2 SUGGESTIONS FOR FURTHER WORK

7.2.1 Applying Pb-free Ternary Solders on Flip Chip Packaging

It is suggested that Pb-free Sn-9Zn binary eutectic solders doped with Al and Cu could be successfully used as solder bumps on chip surface with UBM layer. The size of the solder bump is about 100μm. The reaction between Al and Cu with UBM plays an important role at this level, which determines the reliability of the packaged IC. The effect of Al and Cu on electromigration and the oxidation behavior that may lead to failure is unknown as well.

7.2.2 Determine the Creep Property for Pb-free Ternary Solders

For a low melting point alloy, its creep behavior is important because it is used at high homologous temperature. Solders used in automobiles experience a temperature variation between -40^{0}C and 200^{0}C in winter. Solders in this case are subjected to thermal stress induced by the temperature cycling. Sometimes, creep deformation at the service temperature occurred due to grain-boundary sliding. Thus, it is necessary to check the thermo-mechanical fatigue (TMF) or creep resistance of newly developed ternary and composite solders, to be feasible in long-term use for microelectronic applications.

7.2.3 Reliability Test for Pb-free Ternary Solders

For the long-term reliability of the solder joints in electronic products, an inappropriate joint shape can result in stress concentration at weak points. A deviation from normal solderability can cause severe problems during critical assembly processes. Thus, the solderability of the newly developed Pb-free solders must be investigated in order to prevent the loss or need to rework entire production batches.

7.2.4 Doping of Al and Cu

Since Al and Cu both are easily oxidized and have high melting point, one should think about how to dope these two elements into solder by other methods, rather than alloying. Electroplating and plasma immersion ion implantation may be possible methods to dope these elements into solder. If the doping of Al and Cu into solder bumps can be made practical, then it would increase the feasibility of using Pb-free Sn-9Zn-X ternary solders in the future.

REFERENCES:

1. R. R. Tummala, "Fundamentals of Microsystems Packaging", New York: McGraw Hill, (2001).

2. R R. Tummala, C. P. Wong and Y. C. Chan, "Microelectronic Packaging and Assembly Roadmap for Hong Kong and Pearl River Delta Region: A Team Study and Recommendations", Electronics Packaging Technology Conference, EPA Center, (2000).

3. M. Abtew and G Selvaduray, "Lead-free Solders in Microelectronics", Mater. Sci. and Eng. Rep. 27(5-6), (2000). pp.95-141

4. J. H. Lau, "Handbook of Tape Automated Bonding", New York: Van Nostrand Reinhold, (1992).

5. S. Rudolf, "Surface Mount Technology", Oxford: Butterworth-Heinemann, (1994).

6. K. N. Tu, T. Y. Lee, J. W Jang, L. Li, D. R. Frear, K. Zeng and J. K. Kivilahti, "Wetting Reaction versus Solid State Aging of Eutectic SnPb on Cu", J. Appl. Phys. 89, (2001), pp 4843-4849.

7. J S Hwang, "Modern Solder Technology for Competitive Electronics Manufacturing", New York: McGraw-Hill, (1996).

8. K. N. Tu and K. Zeng, "Tin-Lead (SnPb) Solder Reaction in Flip Chip Technology" Mater. Sci. Eng. R, 34. (2001), pp 1-58.

9. S. C. Johnson, "Electronics: Going 'Green'", Lead-free Electronics, SMT Magazine, November, (2004),

REFERENCES:

1. R. R. Tummala, "Fundamentals of Microsystems Packaging", New York: McGraw Hill, (2001).

2. R. R. Tummala, C. P. Wong and Y. C. Chan, "Microelectronic Packaging and Assembly Roadmap for Hong Kong and Pearl River Delta Region: A Team Study and Recommendations", Electronics Packaging Technology Conference, EPA Center. (2000).

3. M. Abtew and G. Selvaduray, "Lead-free Solders in Microelectronics", Mater. Sci. and Eng Rep. 27(5-6), (2000), pp.95-141.

4. J. H Lau, "Handbook of Tape Automated Bonding", New York: Van Nostrand Reinhold, (1992).

5. S. Rudolf, "Surface Mount Technology", Oxford. Butterworth-Heinemann, (1994).

6. K. N. Tu, T. Y. Lee, I. W. Jang, L. Li, D. R. Frear, K. Zeng and J. K. Kivilahti, "Wetting Reaction versus Solid State Aging of Eutectic SnPb on Cu", J. Appl. Phys. 89. (2001), pp.4843-4849.

7. J. S. Hwang, "Modern Solder Technology for Competitive Electronics Manufacturing", New York: McGraw-Hill, (1996)

8. K. N. Tu and K. Zeng, "Tin-Lead (SnPb) Solder Reaction in Flip Chip Technology" Mater. Sci. Eng. R, 34, (2001), pp.1-58.

9. S C. Johnson, "Electronics Going 'Green'", Lead-free Electronics, SMT Magazine, November. (2004).

http://smt.pennnet.com/Articles/Article_Display.cfm?Section=Articles&Subsection=Display&ARTICLE_ID=216206

10. J. Liu, Lecture note on "Lead-free Solders for Electronics Packaging Application" EPA Centre, City University of Hong Kong. Jan. (2004).

11. "Guidance for Pb-free Soldering Technology", presentation by Tamura Corporation. Tamura Corporation. http://www.tamura-ss.co.jp/en/electric_chemical/guide/2003-07_G-9011.pdf

12. E. R. Monsalve, "Lead ingestion hazard in hand soldering environments", Proceedings of the 8th Annual Soldering Technology and Product Assurance Seminar, February (1984), Naval Weapons Center, China Lake, CA

13. D. Napp, "Lead-free interconnect materials for the electronics industry", Proceedings of the 27th International SAMPE Technical Conference, Albuquerque, NM, 9–12 October (1995), p.342.

14. M. O. Alam, "Study on Interfacial Reactions in Ball-grid-array (BGA) Solder Joints for Advanced Integrated Circuit (IC) Packaging", Ph. D. Thesis, City University of Hong Kong, Hong Kong, (2004).

15. J. Moses, "The Practicing Scientist's Handbook", New York. Van Nostrand Reinhold, (1978).

16. T. C. May and M. H. Woods, "Alpha-particle-induced Soft Errors in Dynamic Memories", IEEE Transactions on Electron Devices, 26(1), (1979), pp.2-9.

17. E P. Wood, and K. L. Nimmo, "In Search of New Lead-free Electronic Solders", J. Electron. Mater. 23(8). (1994), pp.709-714.

18. K. Gerahty, "An update of WEEE and RoHS directives", Circuit World, **29(4)**, (2003).

19. "ASM International, Electronic Material Handbook 1", Materials Park, OH, (1989).

20. C. M. L. Wu, D. Q. Yu, C. M. T. Law and L. Wang, "Properties of lead-free solder alloys with rare earth element additions", Mater. Sci Eng R, **44**, (2004), pp.1-44

21. K. Zeng, and K. N. Tu, "Six Cases of Reliability of Pb-free Solder Joints in Electronic Packaging Technology", Mater. Sci. Eng. R, **38**(2), (2002), pp.55-105.

22. T. P. Vianco, "Development of Alternatives to Lead-bearing Solders, Proceedings of the Technical Program on Surface Mount International", San Jose, CA, Sept., (1993).

23. P. Nash, A Nash, H. Baker et al, "Alloy phase diagrams, ASM Handbook 3", Materials Park, OH, (1990), p.335.

24. A. Sharif, "A Study on Interfacial Interaction Behavior Between Lead-Free Solders and Electroless Nickel Metallization for Advanced Electronic Packaging", Ph. D. Thesis, City University of Hong Kong. Hong Kong, (2005).

25. W. L. Winterbottom, "Converting to Lead-free Solders: an Automobile Industry Perspective", J. Minerals, Metals & Mater. Soc. 45(7), (1993), pp.20-24.

26. J. E Sohn, "Are Lead-Free Solder Joints Reliable?" Circuits Assembly, **13**, (2002), pp.32-36.

27. J. W. Yoon, Y.H. Lee, D. G. Kim, H. B. Kang, S. J. Suh, C. W. Yang, C. B. Lee, J. M. Jung, C. S. Yoo and S. B. Jung, "Intermetallic compound layer growth at the interface between Sn-Cu-Ni solder and Cu substrate", Journal of Alloys and Compounds, **381**, (2004), pp.151-157.

28. P. Nash, A. Nash, H. Baker et al, "Alloy phase diagrams, ASM Handbook 3", Materials Park, OH, (1990), p.37.

29. P. Nash, A. Nash, H. Baker et al, "Alloy phase diagrams, ASM Handbook 3", Materials Park, OH, (1990), p.178.

30. D. S. Dunn, T. F. Marinis, W.M. Sherry and C. J. Williams, "Dependence of Cu/Sn and Cu/60Sn40Pb solder joint strength on diffusion controlled growth of Cu_3Sn and Cu_6Sn_5", Mater. Res. Soc. Symp. Proc. **40**, (1985), pp.129-138

31. R. W. Chuang, S. Choe, and C. C. Lee, "A Fluxless Sn-In Bonding Process Achieving High Re-Melting Temperature", Electronic Components and Technology Conference (2001).

32. S. F. Bartram, W. G. Moffatt and B. W. Roberts, "The In-Sn Phase diagram and superconductivity in In_3Sn", J. Less Common Metal. **62**, (1978), pp.9-12

33. P. Nash, A. Nash, H. Baker et al, "Alloy phase diagrams, ASM Handbook 3", Materials Park. OH, (1990), p.372

34. M. McCormack, S. Jin, "Improved Mechanical Properties in New Pb-free Solder Alloys", J. Electron. Mater. **23**(8), (1994), pp.715-720.

35. M. McCormack, S. Jin, and H. S. Chen, "New Lead-free, Sn-Zn-In Solder Alloys", J. Electron. Mater. **23**(7), (1994), pp.687-690.

36. Y Shi, J. Liu, Y. Yan, Z. Xia, Y. Lei, F. Guo and X Li, "Creep properties of composite solders reinforced with nano- and microsized particles", J. Electron. Mater. 37, (2008), p.507.

37. J. A. Wasynczuk and G.K. Lucey, "Shear Creep of Cu_6Sn_5 Eutectic Composites", Proceedings of the Technical Program, National Electronic Packaging and Production Conference, Anaheim, CA, Cahners Exhibition Group (NEPCON WEST), (Des Plains, IL, 3, 1992), pp 1245-1255.

38. H. S. Betrabet, S. M. McGee and J. K. McKinlay, "Processing Dispersion Strengthened Sn-Pb Solders top Achieve Microstructural Refinement and Stability", Scr. Metall. Mater. 25, (1991), pp.2323–2328.

39. H. Mavoori and S. Jin, "New, creep-resistant, low melting point solders with ultrafine oxide dispersions" J. Electron Mater. 27(11), (1998), pp.1216–1222.

40. J. L. Marshall and J. Calderon, "Hard-particle Reinforced Composite Solders Part 1: Microcharacterisation", Sold. Surf. Mount Technol 9(2), (1997), pp.22-28.

41. J. L. Marshall, J. Sees and J. Calderon, "Microcharacterization of Composite Solders", Proceedings of the Technical Program, National Electronic Packaging and Production Conference, Anaheim, CA, Cahners Exhibition Group (NEPCON WEST), (Des Plains, IL, 3, 1992), pp.1278–1283.

42. J. L. Marshall, J. Calderon, J. Sees, G. Lucey and J S Hwang, "Composite Solders" IEEE Trans. Comp. Hyb. Manufact. Technol. 14(4), (1991), pp.698-702.

43. S. M. L. Sastry, T. C. Peng, R. J. Lederich, K. L. Jerina and C G. Kuo, "Microstructures and Mechanical Properties of In-situ Composite Solders", Proceedings of the Technical Program, National Electronic Packaging and

Production Conference, Anahein, CA, Cahners Exhibition Group (NEPCON WEST), (Des Plains. IL, 3, 1992). p.1266.

44. H. S. Betrabet and S. McGee, "Towards Increased Fatigue Resistance in Sn-Pb Solders by Dispersion Strengthening", Proceedings of the Technical Program, National Electronic Packaging and Production Conference, Anahein, CA, Cahners Exhibition Group (NEPCON WEST), (Des Plains, IL, 3, 1992), pp 1276–1277.

45. R. B. Clough, R. Petel, J. S Hwang and G. Lucey, "Preparation and Properties of Reflowed Paste and Bulk Composite Solder", Proceedings of the Technical Program, National Electronic Packaging and Production Conference, Anahein, CA, Cahners Exhibition Group (NEPCON WEST), (Des Plains, IL, 3, 1992), p 1256.

46. M. McCormack, S. Jin and G.W. Kammlott, "Enhanced Solder Alloy Performance by Magnetic Dispersions", IEEE Trans. Comp. Packag. Manufact Technol.-Part A, **17**(3), (1994) pp.452-457.

47. K. N. Subramanian, T. R. Bieler and J. P. Lucas, "Microstructural Engineering of Solders", J. Electron. Mater. **28**(11), (1999), pp.1176–1183.

48. J. H. Lee, D. J. Park, J. N. Heo, Y. H. Lee, D. H. Shin and Y S. Kim, "Reflow characteristics of Sn-Ag matrix in-situ composite solders" Scr. Mater. **42**(8), (2000), pp.827–831.

49 S. Y. Hwang, J. W Lee and Z. H Lee, "Microstructure of a lead-free composite solder produced by an in-situ process" J. Electron. Mater. **31**(11), (2002), pp.1304–1308.

50. C. G. Guo, S. M. L. Sastry and K. L. Jerina, "Tensile and Creep Properties of In-Situ Composite Solders", Proceedings of the 1st International Conference

on Microstructural and Mechanical Properties of Aging Materials—Proceedings of Minerals, Metals and Materials Society (TMS) Symposium, (Chicago, IL), (1993), pp.409–415

51. C. G. Guo, S. M. L. Sastry and K. L. Jerina, "Fatigue Deformation of In-Situ Composite Solders", Proceedings of the 1st International Conference on Microstructural and Mechanical Properties of Aging Materials—Proceedings of Minerals, Metals and Materials Society (TMS) Symposium, (Chicago, IL), (1993), pp. 417–423.

52. S. Choi, T. R. Bieler, J. P. Lucas and K. N. Subramanian, "Characterization of the growth of intermetallic interfacial layers of Sn-Ag and Sn-Pb eutectic solders and their composite solders on Cu substrate during isothermal long-term aging". J. Electron. Mater. 28(11). (1999). pp.1209–1215.

53. S. Choi, J. P. Lucas, K. N. Subramanian and T. R. Bieler, "Formation and growth of interfacial intermetallic layers in eutectic Sn-Ag solder and its composite solder joints", J. Mater. Sci.-Mater. El. 11(6), (2000), pp.497–502

54. F. Guo, S. Choi, J. P. Lucas and K. N. Subramanian, "Microstructural characterization of reflowed and isothermally-aged Cu and Ag particulate reinforced Sn-3.5Ag composite solders", Sold. Surf. Mount Technol. 13(1). (2001). pp.7–18.

55. F. Guo, J. Lee, S. Choi, J.P. Lucas, T.R. Bieler and K.N. Subramanian, "Processing and aging characteristics of eutectic Sn-3.5Ag solder reinforced with mechanically incorporated Ni particles", J. Electron. Mater. 30(9), (2001), pp.1073–1082.

56. I. E. Anderson, J. C. Foley, B.A. Cook, J. Harringa, R.L. Terpstra, and O. Unal, "Alloying Effects in Near-eutectic Sn-Ag-Cu Solder Alloys for

Improved Microstructural Stability", J. Electron. Mater. 30(9), (2001), pp.1050-1059.

57. K. S. Kim, S. H. Huh and K. Suganuma, "Effect of Fourth Alloying Additive on Microstructures and Tensile Properties of Sn-Ag-Cu Alloy and Joints with Cu", Microelectronics Reliability, 43, (2003), pp.259-267.

58. X. L. Zhong and M. Gupta, "High Strength Lead-Free Composite Solder Materials using Nano-Al_2O_3 as Reinforcement", Adv. Eng. Mater. 7(11), (2005), pp.1049–1054.

59. K. Seeling, "A Study of Lead-Free Solder Alloys", Technology at AIM. Inc., in Cranston, RI, 1(1), (1995).

60. Y. Zhang, T. Liang and M. A. Jusheng, "Phase diagram calculation on Sn–Zn–Ga solders", J. Non-Crystall. Solid. 336, (2004), pp.153–156.

61. S. Vaynman and M. E. Fine, "Development of fluxes for lead-free solders containing zinc" Scr. Mater. 41, (1999), pp.1269-1271.

62. X. Chen, M. Li, X. X. Ren, A. M. Hu and D. L. Mao, "Effect Of Small Additions Of Alloying Elements On The Properties Of Sn-Zn Eutectic Alloy", J. Electron. Mater. 35(9), (2006), pp.1734-1739.

63. C. M. Chuang, T. S. Lui and L. H. Chen, "Effect of aluminum addition on tensile properties of naturally aged Sn-9Zn eutectic solder", J. Mater. Sci. 37, (2002), pp.191-195.

64. A. Sebaoun, D. Vincent and D. Treheux, "Al-Zn-Sn Phase Diagram-Isothermal Diffusion in Ternary System", Mater Sci Tech. 3(4), (1987), pp.241-248.

65. K. L. Lin, L. H. Wen and T. P. Liu, "The Microstructures of the Sn-Zn-Al Solder Alloys", J. Electron Mater. **27**(3), (1998), pp.97-105.

66. H. P. Xie. D. Q. Yu and L. Wang, "Effects of Bi, Ni additives on the microstructures and wetting properties of Sn-Zn-Cu lead-free alloy", Proceedings of the International Conference on Asian Green Electronics, (2005).

67. Z. Xiaoyan. Mr. Z. Qun, X. C. Wang and W. T Zhang, "Influence of Cu, Ce on Physics and Chemistry Properties of Sn-Zn System Solder Alloys", New technologies and process, **1**, (2007).

68. T. Ichitsubo, E. Matsubara, K. Fujiwara. M. Yamaguchi, H. Irie, S. Kumamoto and T. Anada, "Control of compound forming reaction at the interface between SnZn solder and Cu substrate", J. Alloy. Comp. **392**, (2005), pp.200–205.

69. L. Wang, H. T. Ma and H. P. Xie, "Interfacial Reaction and Shear Strength of Sn-Zn-Cu/Cu Joints", J. Dalian Uni. Tech. **45**(5), (2005), pp.663-667.

70. S. W. Chen, C. C. Lin and C. M Chen, "Determination of the Melting and Solidification Characteristics of Solders Using Differential Scanning Calorimetry", Metall. Mater Trans A, **29**, (1998), pp.1965-1972.

71. Manual, DSC Q-10 Differential Scanning Calorimeter.

72. J. G. Maveety, P. Liu, J. Vijayen, F. Hua and E. A. Sanchez, "Effect of Cooling Rate on Microstructure and Shear Strength of Pure Sn, Sn-0.7Cu, Sn-3.5Ag, and Sn-37Pb Solders" J. Electron. Mater. 33(11), (2004), pp.1355-1362.

73. D. Frear, H. Morgan, S. Burchett and J. Lau, "The Mechanics of Solder Alloy Interconnects", New York: Van Nostrand Reinhold, (1994).

74. S. N. Salama and H. A. El-Batal, "Microhardness of phosphate glasses", J. Non-Crystall. Solid. 168(1-2), (1994), pp.179-185.

75. H. Buckle, "Progress in micro-indentation hardness testing", Met. Rev. 4, (1959), pp.49–100.

76. I. S. Virk, M. B. Winnicka and R. A. Varin: "Dependence of vickers microhardness on load in the $L1_2$ titanium and zirconium ternary trialuminides", Scr. Metall., 24, (1990), pp.2181-2185.

77. F. A. Mcclintock and A. S. Argon, "Mechanical Behavior of Materials", Massachusetts: Addison-Wesley, Reading, (1996), p. 458.

78. M. A. Meyers and K. M. Chawla, "Mechanical Metallurgy-Principles and Applications", New Jersey: Prentice-Hall, Englewood Cliffs, (1984).

79. G. E. Dieter, "Mechanical Metallurgy", New York: McGraw-Hill, (1986).

80. M. Braunovic, Proceedings of the International Symposium on Science Hardness Testing and its Research Applications, Detroit, USA, October, (1971).

81. W. D. Callister, "Materials Science and Engineering an Introduction", Canada: John Wiley & Sons Inc. 4th Edition, (1996).

82 J E. Lee, K. S. Kim, M. Inoue. J Jiang and K. Suganuma, "Effects of Ag and Cu addition on microstructural properties and oxidation resistance of Sn–Zn eutectic alloy", J. Alloy. Comp. **454**, (2008), p.310.

83. K. L. Lin and C. L. Shih, "Wetting interaction between Sn-Zn-Ag solders and Cu", J Electron. Mater. **32**, (2003), p.95.

84 A. Sharif and Y. C. Chan, "Effect of reaction time on mechanical strength of the interface formed between Sn-Zn (-Bi) solder and Au/Ni/Cu bond pad" J. Electron. Mater. **35**, (2006), p.1812